applied physics, faculty of applied sciences, TU Delft

Correcton Method for Neutron Transport Calculations with Real Time Flux Estimation

Bachelor thesis

Name:	Hennink, Aldo
Student Number:	1513222
Supervisors:	dr. ir. Eduard Hoogenboom, department: PNR
	Bart Sjenitzer, MSC
Starting Date:	September 22, 2011
Final Date:	March 1, 2012

Not Confidential

Correcton Method for Neutron Transport Calculations with Real Time Flux Estimation

Hennink, Aldo

March 1, 2012

Abstract

A new self-learning Monte Carlo technique is presented that enhances source convergence in loosely coupled systems. It uses correctons in combination with an estimate of the neutron flux, resulting in a particle flux with little or no spatial variation. The estimate is obtained in real time, i.e.: during the calculation. Therefore, no prior Monte Carlo simulations or deterministic calculations are necessary.

The method solves the source convergence problem for several simplified systems of fuel assemblies for which a conventional calculation with neutrons fails.

Contents

Chapter 1

Introduction

In order to analyse engineering problems related to neutron transport, numerical methods are needed. One of those is the Monte Carlo method, which is based on approximating a deterministic quantity by performing random experiments.

In a Monte Carlo criticality calculation, one performs an iteration that must converge after some amount of cycles. For some physical systems, this does not happen. Also, accurate estimates of the neutron flux can sometimes be very time-consuming.

Both of these problems could be solved by the correcton method. Unfortunately, an estimate of the neutron flux is often needed in advance. This estimate can be obtained from another (less extensive) Monte Carlo calculation, or by using more conventional means.

This thesis explores the possibility of a 'real time' neutron flux estimation during a correcton calculation. That is, the neutron flux estimate is adjusted and refined during the calculation.

This thesis is submitted as a partial fulfilment of the bachelor of physics education program of the technical university of Delft.

1.1 Setup of this thesis

This thesis should be readable to anyone with a Bachelor's degree in physics, while at the same time containing sufficient new or advanced material to keep physicists in the relevant field interested. To facilitate this, two introductory chapters have been added.

Chapter 2 deals with some basic, essential results from nuclear reactor physics. Chapter 3 (especially sections 3.1 through 3.7) introduces the general concept of the Monte Carlo method, its applicability to nuclear calculations and some of the standard variance reduction methods, without containing any previously unknown material. Anyone already familiar with parts of it can simply skim through the sections he or she already knows.

Appendix A contains a formal setup of probability theory and Markov chains, which may be new to some.

When introducing the Monte Carlo method in chapter 3, it would have been easiest to simply start with a particle perspective of neutron transport. That way, simulating neutrons would instantly seem intuitive and the mathematics is almost unnecessary. (This is done in Hoogenboom et. al. [1].)

Instead, the neutron transport equation and the concept of reaction rate densities from chapter 2 are taken as axioms from which a new formulation of the neutron transport equation can be derived. Only then is the validity of the Monte Carlo method for estimating quantities demonstrated.

There are two principle reasons for this choice of presenting the material. First, chapter 3 is mostly aimed at physicist who are already quite familiar with the neutron transport equation, but have no experience in Monte Carlo calculations. Perhaps more importantly, the intuitive understanding of simulated neutrons does not apply to the simulation technique using correctons that is introduced in chapter 4. The slightly more abstract treatment in chapter 3 should make the validity of the correcton method obvious at first sight.

1.2 Acknowledgement

Ending on a more personal note, I would like to thank Bart Sjenitzer for letting me use his omniscience in the field of Monte Carlo methods in nuclear computing and introducing me to the world of Fortran, Linux, clusters and really just computers in general. My gratitude also goes out to the folks at R^3, TU Delft and PNR in particular, for making my short stay at their department fun.

Chapter 2

Introduction to Nuclear Reactor Physics

2.1 Nuclear reactions

If an atomic nucleus collides with another nucleus or a subatomic particle, it might produce particles that are different from the initial particles. Such an event is referred to as a **nuclear reaction**. Compared to some charged subatomic particles, neutrons can interact with nuclei relatively easily, since they are not repulsed by the positive charge of the nucleus or the negative charge of the electrons. Here the focus of the discussion will lie on the different types of interaction neutrons can have with nuclei.

(Nuclear) fission is a nuclear reaction in which a large nucleus splits into smaller parts. This is accompanied by a (large) release of energy and the production of subatomic particles, such as neutrons and photons. In the event of **neutron capture**, the neutron will be assimilated by the nucleus to form a heavier nucleus. Sometimes the heavier nucleus is unstable, in which case it will decay.

Fission and capture are both examples of **absorption**, meaning that the neutron seizes to exist as an individual particle. Conversely, in a **scattering reaction** the neutron remains an unbound particle, but it is forced to deviate from a straight path by the nucleus. One can make a distinction between elastic and inelastic scattering[1], based on whether the kinetic energy of the neutron is conserved. ([2], 12-16)

The number of neutrons in any macroscopic material is too large to keep track of the individual particles. Therefore, statistics are used to describe the behaviour of all neutrons combined. To quantify the probability of certain nuclear interactions, consider the following scenario.

A beam of neutrons with the same speed, energy and direction has a uniform intensity (I) and is incident normally upon the surface of a plane. On the plane, a constant number of nuclei per area (N_A) are located. Define the **reaction rate** $R_{\langle j \rangle}$ as the amount of nuclear reactions of type $\langle j \rangle$ that take place per

[1] Actually one might argue that elastic scattering is not a nuclear reaction, since the none of the particles changes. [3]

unit of time per area. Since the nuclei are all on the same plane, they cannot 'shield' each other from being hit by a neutron. Therefore $R_{\langle j \rangle}$ will simply be proportional to I and N_A. The constant of proportionality is called the **microscopic cross section** for reaction type $\langle j \rangle$, denoted by $\sigma_{\langle j \rangle}$:

$$R_{\langle j \rangle} = \sigma_{\langle j \rangle} I N_A.$$

Obviously, the total probability of a nuclear reaction occurring is the sum over all individual probabilities of a specific reaction. Therefore, the cross section corresponding to *any* nuclear reaction equals the sum over all individual microscopic cross sections. This quantity is referred to as the *total* microscopic cross section, denoted by σ_T.

The concept of cross sections can be extended to three dimensions by considering an incident beam of neutrons on a three-dimensional object. Part of the neutrons will collide with the first nuclei, whilst others will travel deeper into the material. Suppose x is the distance the neutron beam has travelled in the material. Then the intensity I of the beam is a function of x. The probability of colliding with a nucleus at any point does not depend on the amount of nuclei that have already been passed, so an exponential relationship between I and x is to be expected.

The amount of neutrons that react in the region between x and $x + dx$ is $\sigma_T I N$, where N is the number of nuclei per unit volume. This implies that

$$dI(x) = -\sigma_T N I(x) dx. \tag{2.1}$$

Solving Eq. (2.1) and setting $I(x = 0) = I_0$ leads to

$$I = I(x) = I_0 \exp\left[-N\sigma_T x\right].$$

The **macroscopic cross section** corresponding to a nuclear reaction of type $\langle j \rangle$, denoted by $\Sigma_{\langle j \rangle}$, is now defined as

$$\Sigma_{\langle j \rangle} \equiv N \sigma_{\langle j \rangle}. \tag{2.2}$$

If a material consists of more than one type of material, the effective cross section is the weighted average of the cross sections of the different materials.

Note that Eq. (2.1) can be rewritten to find the relative decrease of intensity over a distance dx:

$$\frac{\left(\frac{dI}{I}\right)}{dx} = -\Sigma_T.$$

This means that Σ_T can be interpreted as the probability per unit length that a neutron will collide with a nucleus. The probability that a neutron will travel a distance d without engaging in a nuclear reaction is therefore just

$$\mathbb{P}\left[\text{no interaction after travelling a distance } d\right] = \exp\left(-\Sigma_T d\right).$$

The probability density function for the distance travelled before undergoing a reaction is

$$p(d) = \Sigma_T \exp\left(-\Sigma_T d\right) \ , \ d > 0 \tag{2.3}$$

and the average distance travelled before colliding is $\mathbb{E}\left[d\right] = 1/\Sigma_T$. ([2], 16-22)

2.2 Neutron Transport

The **neutron density** N is defined by the relation

$$N(\vec{r},t)d^3r \equiv \text{expected number of neutrons in volume } d^3r \text{ at } \vec{r} \text{ at time } t.$$

This does not take into account the fact that neutrons are discrete particles. Instead, the neutron density is, in general, a continuous function of position. Also, the statistical nature of the problem at hand is ignored. In the following discussion, the neutron density is assumed to be a deterministic function. In reality, however, it is a stochastic variable. The goal in neutron transport theory is to find the neutron density at any given position and time. ([2], 105)

Suppose a neutron has a (scalar) speed v. Since $\Sigma_{\langle j \rangle}$ is the probability the neutron will engage in a reaction of type $\langle j \rangle$ with a nucleus per unit length the neutron travels, the frequency at which a single neutron has such a reaction is $v\Sigma_{T\langle j \rangle}$. (This is also called the **reaction frequency**.) The **reaction rate density** F is the reaction frequency multiplied by the neutron density:

$$F_{\langle j \rangle}(\vec{r},t) \equiv v\Sigma_{\langle j \rangle}N(\vec{r},t). \tag{2.4}$$

$F_{\langle j \rangle}(\vec{r},t)d^3r$ is the total frequency at which interactions of type $\langle j \rangle$ are occurring at $\vec{r}$ in volume d^3r at time t. ([2], 21, 105)

Apparently, the reaction rate depends on the product $vN(\vec{r},t)$. In fact, this quantity has a name of its own: the **(scalar) neutron flux**, defined by

$$\phi(\vec{r},t) \equiv vN(\vec{r},t). \tag{2.5}$$

The name is a bit misleading, since it is entirely different from the usual 'fluxes' in electromagnetics or fluid mechanics. This flux is a scalar quantity and doesn't say anything about the direction in which the neutrons are moving.

The information about the direction of the neutron flow is contained in the (unit) **direction vector** $\hat{\Omega}$. Instead of using the neutron speed, it is customary to specify the energy E, which relates to the speed in the classical way. By distinguishing between neutrons with different energy and direction, one can decompose the neutron density into the **angular neutron density** $n(\vec{r},t,E,\hat{\Omega})$.[2] The interpretation is that $n(\vec{r},t,E,\hat{\Omega})d^3rdEd\hat{\Omega}$ is the number of neutrons in a volume d^3r, in an energy range dE and in a solid angle $d\hat{\Omega}$ at $\vec{r}$, E and $\hat{\Omega}$ respectively.

A systematic way to derive the equation that describes the angular neutron density is to work out the balance equation for a volume of arbitrary shape. Since this equation is valid for any arbitrary volume $\mathcal{V}$ in space, the usual argument

$$\int_{\mathcal{V}} f(\vec{r}) = 0 \Rightarrow f(\vec{r}) = 0$$

can be used to derive a differential equation for the neutron density at any point.

All this is done in Duderstadt et al. ([2], 111-114). Here only the result is

[2] It suffices not to consider the complete quantum mechanical state (which would, amongst others, include spin), but instead to treat the neutrons as classical particles.

given, with some explanation of where the terms come from.

$$\begin{aligned}\frac{\partial n}{\partial t} &= -\underbrace{v\hat{\Omega}\cdot\nabla n(\vec{r},E,\hat{\Omega},t)}_{[1]} - \underbrace{v\Sigma_T n(\vec{r},E,\hat{\Omega},t)}_{[2]} \\ &+ \underbrace{\int_{(\hat{\Omega}',E')\in(<4\pi>,\mathbb{R}^+)} v'\Sigma_s(E'\to E,\hat{\Omega}'\to\hat{\Omega})n(\vec{r},E',\hat{\Omega}',t)\ \mathrm{d}(\hat{\Omega}',E')}_{[3]} \\ &+ \underbrace{S(\vec{r},E,\hat{\Omega},t)}_{[4]} \end{aligned} \tag{2.6}$$

The terms represent respectively:

1. neutrons entering and leaving the point in space due to the neutron flux;
2. neutrons with $E, \hat{\Omega}$ entering a collision at $\vec{r}$ (they change their direction and/or energy and thus no longer contribute to $n(\vec{r}, E, \hat{\Omega}, t)$);
3. **inscattering**: neutrons that have a collision at $\vec{r}$ and change their direction and energy to $\hat{\Omega}$ and E. Here $\Sigma_s(E' \to E, \hat{\Omega}' \to \hat{\Omega})$ represents the cross section that corresponds to the event that a neutron with $\hat{\Omega}', E'$ scatters to $\hat{\Omega}, E$;
4. the source term. It represents all neutrons that come to life at time t and position $\vec{r}$ with energy E and direction $\hat{\Omega}$. This includes both neutrons that are created in a fission reaction and neutrons that are emitted by an external source.

Not surprisingly, Eq. (2.6) is known as the **neutron transport equation**. It is reminiscent of the Boltzmann equation. Unfortunately, it usually cannot be solved analytically, so simplifications or numerical methods are necessary.

2.3 Criticality

In a fission reaction, new neutrons are created. In turn, some of these neutrons may engage in a fission reaction, to create more neutrons. This way, a chain reaction can occur. If a neutron generates, on average, more than one new neutron, the total amount of neutrons will increase. If a neutron creates less then one new neutron on average, the chain reaction will gradually die out. The former case is referred to as **supercritical**, while the latter is **subcritical**. A system is **critical** if the number of neutrons remains the same.

To quantify these ideas, the multiplication factor k is introduced:

$$k \equiv \frac{\text{rate of neutron production}}{\text{rate of neutron loss (due to leakage from the system and absorption)}}$$

To perform a direct calculation of k, one could try to approximate the neutron transport Eq. (2.6) directly with a standard multigrid method. Needless to say, this is computationally demanding. (There are seven independent variables to be taken into account.) Also, the discretisation introduces a bias and the method may turn out to be unstable.

Another approach would be to calculate the expected number of fission neutrons a neutrons creates in a system. That would include determining

- the probability that a neutron leaks out of the system before absorbing in the system;
- the probability a neutron will be absorbed in the parts of the system where fission can occur (the **fuel**), conditional on being absorbed in the system;
- the probability of fission, conditional on absorption in the fuel;
- the average amount of neutrons produced in a fission reaction.

This is not a trivial task and things get even more complicated when taken into account the fact that neutrons may only fission at low energy, whilst they are 'born' at high energy. ([2], 74-86)

The numerical approach that will be used here is the **source iteration** method (a variation on the **power method**) in combination with the Monte Carlo method. This will be explained in sections 3.2 through 3.5.

Chapter 3

Monte Carlo Method for Neutron Transport and Criticality Calculations

3.1 Introduction to the Monte Carlo method

In general, the Monte Carlo method uses a stochastic process to solve a deterministic problem.[1] Basically, it can be summarised as follows. Suppose one wants to approximate a variable $\mathbf{x}$.[2] Now the Monte Carlo Method usually consists of the following steps.

1. *Find some stochastic process that has realisations θ_i, with $\mathbb{E}[\theta_i] = \boldsymbol{x}$.*

   This may already seem like an big limitation to the practical uses of the Monte Carlo method. However, with some creativity a surprisingly large variety of problems can be reduced to finding the expectation value of a stochastic process. In fact, the Monte Carlo method has an amazingly wide range of possible applications in engineering, science, finance, mathematics, biology and even game theory.

   In sections 3.2 through 3.4 it will be shown that there is a very natural stochastic process that can be applied to approximate the Boltzmann Equation.

2. *Sample realisations of θ_i using the probability distribution of the previous step.*

   Nowadays, this will usually be done using a computer and a random number generating algorithm. The ability to generate large quantities of pseudo-random numbers and the the enormous increase in computational power over the last decades have facilitated the usage of Monte Carlo methods for many practical applications.

   A very brief overview of random sampling from a probability density function can be found in appendices B.1 and B.2.

[1] ref. appendix A.1 for a review of probability theory

[2] Note that $\mathbf{x}$ can, in general, have any shape or form: real, complex, scalar, vector, ...

3. *Approximate* $\boldsymbol{x}$ *by using the Law of Large Numbers.*

   Somewhat heuristically, the Law of Large Numbers states that for an infinite number of samples $\theta_1, \theta_2, \theta_3, ...$, the average value of the samples converges almost surely to the expectation value. That is, if the θ_i are **independent, identically distributed (i.i.d.)**, then

$$\mathbb{P}\left[\lim_{h\to\infty}\frac{1}{h}\sum_{i=1}^{h}\theta_i = \mathbf{x}\right] = 1\ .$$

   where $\mathbb{P}[-]$ is the probability operator (appendix A.1).

   In reality, there will only be a finite number $N \in \mathbb{N}$ of samples. This is where the approximation part of the Monte Carlo method comes in:

$$\mathbf{x} \simeq \frac{1}{N}\sum_{i=1}^{N}\theta_i. \tag{3.1}$$

The Law of Large Numbers guarantees stable long-term results for the Monte Carlo method. However, it doesn't state anything about the accuracy of formula (3.1). To determine a confidence interval for $\mathbf{x}$, the **Central Limit Theorem** can be used. It states that, given a sequence $\{Q_i\}$ of N continuous i.i.d. random variables, the distribution of $\sum_i Q_i$ approaches a normal (Gaussian) distribution for $N \to \infty$. More precisely,

$$\mathbb{P}\left[\sqrt{N}\left(-\mathbb{E}\left[Q\right] + \frac{1}{N}\sum_{k=1}^{N}Q_k\right)\right](u) \overset{N\to\infty}{\longrightarrow} \mathcal{N}(0, \mathrm{Var}(Q), u),$$

where

$$\mathcal{N}(\mu, \sigma^2, x) = \frac{1}{\sqrt{2\pi\sigma^2}}\exp\left(-\frac{(x-\mu)^2}{2\sigma^2}\right).$$

The distribution of the sum of a large sample of random variables can therefore be approximated by a normal distribution. In general, this is a better approximation if N is large and if the Q_j don't have a very skewed probability density function.

3.2 Rewriting the neutron transport equation

In this thesis all quantities will be considered to be time-independent. (This is common in nuclear reactor analysis.) In a steady-state system, the angular neutron density is constant in time, so the transport and production terms in the neutron transport Eq. (2.6) must balance each other out.

To implement the Monte Carlo method in neutron transport calculations, neutron transport must first be described in a different manner from section 2.2. To this end, some new quantities are introduced:

the state $P \equiv (\vec{r}, E, \hat{\Omega})$: a short-hand notation for the position, energy and direction;

the collision density $\psi(P)$: the reaction rate density of collisions where the neutron entering the collision has a state P;

the emission density $\chi(P)$: the reaction rate density of neutrons leaving a collision or a source in a state P;

the transition kernel $T(\vec{r}\,' \to \vec{r}, E, \hat{\Omega})$, implicitly defined as

$$\int_{\mathbb{R}^3} T(\vec{r}\,' \to \vec{r}, E, \hat{\Omega}) \chi(\vec{r}\,', E, \hat{\Omega}) \, \mathrm{d}\vec{r}\,' = \psi(\vec{r}, E, \hat{\Omega}); \tag{3.2}$$

the collision kernel $C(\vec{r}, E' \to E, \hat{\Omega}' \to \hat{\Omega})$, implicitly defined as

$$\int_{4\pi} \int_{\mathbb{R}^+} \psi(\vec{r}, E', \hat{\Omega}') C(\vec{r}, E' \to E, \hat{\Omega}' \to \hat{\Omega}) \, \mathrm{d}E' \mathrm{d}\Omega' = \chi(\vec{r}, E, \hat{\Omega}) - S(\vec{r}, E, \hat{\Omega}). \tag{3.3}$$

Note that $\chi(\vec{r}, E, \hat{\Omega}) - S(\vec{r}, E, \hat{\Omega})$ is the reaction rate density that corresponds to particles leaving a collision.

For future reference, it is worth noting that by inserting equation (3.2) in Eq. (3.3), $\chi(\vec{r}, E, \hat{\Omega}) - S(\vec{r}, E, \hat{\Omega})$ can also be computed as

$$\chi(P) - S(P) = \int T(\vec{r}\,' \to \vec{r}, E', \hat{\Omega}') \; C(\vec{r}, E' \to E, \hat{\Omega}' \to \hat{\Omega}) \chi(P') \, \mathrm{d}P'; \tag{3.4}$$

the K-transport kernel $K(P' \to P)$:

$K(P' \to P) \equiv T(\vec{r}\,' \to \vec{r}, E', \hat{\Omega}') \; C(\vec{r}, E' \to E, \hat{\Omega}' \to \hat{\Omega})$;

the L-transport kernel $L(P' \to P)$:

$L(P' \to P) \equiv C(\vec{r}\,', E' \to E, \hat{\Omega}' \to \hat{\Omega}) T(\vec{r}\,' \to \vec{r}, E, \hat{\Omega})$.

At the risk of being slightly pedantic, it must be emphasised that none of the statements above require the existence of individual particles (neutrons) in order to make sense. (All quantities take on a value in a continuous range of real numbers.)

The goal of the following analyses is to derive a general expression for the collision density in terms of the other quantities. Since it relates to the neutron flux in a very simple manner via Eq. (2.4), finding the collision density is equivalent to solving the neutron transport Eq. (2.6).

Substituting Eq. (3.3) in (3.2) results in

$$\begin{aligned} \psi(\vec{r}, E, \hat{\Omega}) \quad &= \quad \int_V T(\vec{r}\,' \to \vec{r}, E, \hat{\Omega}) \; [\; S(\vec{r}\,', E, \hat{\Omega}) \\ &+ \quad \int_{4\pi} \int_{\mathbb{R}^+} \psi(\vec{r}\,', E', \hat{\Omega}') C(\vec{r}\,', E' \to E, \hat{\Omega}' \to \hat{\Omega}) \, \mathrm{d}E' \mathrm{d}\Omega' \;] \, \mathrm{d}V'. \end{aligned}$$

Noting that $T(\vec{r}\,' \to \vec{r}, E, \hat{\Omega})$ is not a function of E' or $\hat{\Omega}'$ and recalling the definition of the L-transport kernel, this can be simplified to

$$\psi(P) = \int_V T(\vec{r}\,' \to \vec{r}, E, \hat{\Omega}) S(\vec{r}\,', E, \hat{\Omega}) \, \mathrm{d}\vec{r} + \int L(P' \to P) \psi(P') \, \mathrm{d}P'. \tag{3.5}$$

The collision density can be decomposed into several components that correspond to different amounts of collisions since emission from a source:

$$\psi(P) = \sum_{i=0}^{\infty} \psi_i(P), \tag{3.6}$$

where $\psi_l(P)$ is the reaction rate density for collisions in which the neutron entering the collision has had l previous collisions. ([4], 11-12) The sum of the (direct) contributions of the sources to $\psi(P)$ is simply $\psi_0(P)$:

$$\psi_0(P) = \int_V T(\vec{r}\,' \to \vec{r}, E, \hat{\Omega}) S(\vec{r}\,', E, \hat{\Omega}) \, \mathrm{d}\vec{r}\,'. \tag{3.7}$$

Of course, collisions corresponding to $\psi_{n+1}(P)$ are a result of collisions corresponding to $\psi_n(P)$. This implies that $\psi_{n+1}(P)$ depends on $\psi_n(P)$ via Eq. (3.5), where it should be noted that the source has no (direct) contribution to $\psi_n(P)$ for $n \geq 1$.

$$\psi_{n+1}(P) = \int_{(\mathbb{R},\mathbb{R}^+,\langle 4\pi \rangle)} \psi_n(P') L(P' \to P) \, \mathrm{d}P' \qquad \forall \, n \in \mathbb{N}\backslash\{0\}$$

By means of induction, a direct formula for ψ_k can now be found:

$$\psi_k(P) = \int \dots \int \left(\psi_0(P_0) \prod_{x=0}^{k-1} L(P_x \to P_{x+1}) \right) \prod_{y=0}^{k-1} \mathrm{d}P_y.$$

Finally, recalling Eq. (3.6),

$$\psi(P) = \psi_0(P) + \sum_{k=1}^{\infty} \left[\int \dots \int \left(\psi_0(P_0) \prod_{x=0}^{k-1} L(P_x \to P_{x+1}) \right) \prod_{y=0}^{k-1} \mathrm{d}P_y \right], \tag{3.8}$$

where $\psi_0(P)$ is given by Eq. (3.7).

In and of itself, this is quite an achievement. For example, if S does not depend on ψ (i.e.: if there is no fission and only an external source), a direct computation of the collision density is now possible using equations (3.7) and (3.8).

Note ψ, and thus the neutron flux, are only determined up to an integration constant. In the rest of this thesis, two fluxes are considered equivalent if they are a multiple of each other.

The problem, of course, is that conventional numerical methods for integrating over many dimensions are clumsy at best. Fortunately, it is in the evaluation of such integrals in hyperspace that the Monte Carlo method thrives. To implement a Monte Carlo analysis, a radically new interpretation of the transition and collision kernels is necessary. (The reader is advised to review appendix A at this point.)

First make a few observations:

1. There are no negative angular neutron fluxes or reaction rates. Therefore, T and C are always either positive or zero, and thus the same holds for the K- and L-transport kernels.

2. Both the energies E and E' and the directions $\hat{\Omega}$ and $\hat{\Omega}'$ in $C(\vec{r}, E \to E', \hat{\Omega} \to \hat{\Omega}')$ will always lie in $\hat{\Omega}, E$-space. Also, $\vec{r}, \vec{r}' \in \mathbb{R}^3$ in $T(\vec{r} \to \vec{r}\,', E, \hat{\Omega})$.

   K and L can therefore both be viewed as functions that map a point in P-space to another point in P-space.

3. Eq. (3.2) is linear. Specifically, it is additive: if ψ_1 and ψ_2 are solutions to χ_1 and χ_2 respectively, then $\psi_1 + \psi_2$ will be the solution to $\chi_1 + \chi_2$. Therefore, T is a function that maps a point from position space to another point in position space.

   Similarly, from its definition (3.3), it follows that C is an additive kernel that maps a point from $E, \hat{\Omega}$-space to another point in $E, \hat{\Omega}$-space.

   Therefore, both K and L are additive as well.

Next, define a probability space with the whole of P-space as its sample space. It now becomes apparent that the statements above are equivalent to the Kolmogorov axioms from appendix A.1 if T and C (and thus K and L) are regarded as (joint) probability density functions. A point in P-space satisfies Eq. (A.1) and is thus a stochastic variable. The process $(P_0, P_1, \ldots)$ is therefore a time-homogeneous Markov chain (appendix A.2).

This justifies the use of the Monte Carlo method to approximate ψ. That is, if the source distribution is known, the collision density can be found by sampling from the kernels in equations (3.7) and (3.8).

3.3 Source iteration

If the average number of new fission particles per collision reaction is known and there are no external sources, then S can be found from ψ. The problem is that S is, in turn, needed to approximate ψ. To solve this issue, the Markov chain Monte Carlo method (a variation on the power method) is used. (Readers unfamiliar with this are referred to appendix A.2.)

First, sample from a homogeneous source distribution $S^{(0)}$.[3] Now use this distribution to calculate a collision density $\psi^{(1)}$. Next, use $\psi^{(1)}$ to calculate a new source distribution $S^{(1)}$, which is used to determine a collision density $\psi^{(2)}$, and so on and so forth. Since $S^{(n)}$ depends solely on $\psi^{(n)}$, which depends solely on $S^{(n-1)}$, the stochastic process $(S^{(0)}, S^{(1)}, \ldots)$ is a Markov chain.

If the system is critical and $S^{(n)}$ is the *actual* source, then $S^{(n+1)} = S^{(n)}$. Therefore, the real source distribution is the stationary distribution of the Markov process. From equations (A.2) and (A.3) it follows that it must also be the limiting distribution. The limiting distribution can be approximated by $S^{(I)}$ for some large I.

Obviously, this will not work well if the system isn't critical, but there's a method of solving this, as will be explained in section 3.5.

[3] Actually *any* distribution should do, though it seems best not to start with a point source. [5]

The process of simulating the Markov chain and letting it converge to S is called **source iteration** or **source convergence**. Every step in the Markov chain is called a **cycle**. To avoid the enormous computational effort of having to perform the source iteration many times, many source distributions in the set $\{S^{(m)}, m \geq I\}$ are used in a Monte Carlo calculation. These are referred to as the **inactive cycles**. The rest of the cycles are called **active**.

3.4 Particle histories

3.4.1 Sampling from the kernels

$\chi(P)$ can be written as a weighted linear combination of hyper-dimensional Dirac delta functions $\delta(P)$ in P-space. ($\chi(P) \equiv \int \chi(P')\delta(P' - P)\ \mathrm{d}P'$) Recall that the equation that defines the transition kernel T is linear. Therefore, in order to determine how to sample from the transition kernel, it suffices to consider only the case that $\chi(\vec{r}, E, \hat{\Omega}) = \delta(\vec{r}^*, E, \hat{\Omega})$ for an arbitrary $(\vec{r}^*, E, \hat{\Omega})$.

The physical interpretation of this situation would be that there is a single particle that leaves a collision or source (i.e.: start a flight path) in the state $(\vec{r}^*, E, \hat{\Omega})$. ψ would then be the collision density resulting from a single neutron that starts a flight path.

From Eq. (3.2), the collision density is

$$\psi(\vec{r}, E, \hat{\Omega}) = T(\vec{r}^* \to \vec{r}, E, \hat{\Omega})\ .$$

(The particle is 'smeared out' over P-space.)

Since the transition kernel $T(\vec{r}^* \to \vec{r}, E, \hat{\Omega})$ can be interpreted as a probability density function, it can be sampled by assigning probabilities to the event of a single neutron starting a trajectory at $(\vec{r}^*, E, \hat{\Omega})$ to have its next collision in $\mathrm{d}\vec{r}, \mathrm{d}E, \mathrm{d}\hat{\Omega}$ at $(\vec{r}, E, \hat{\Omega})$.

In fact, by a similar reasoning, one can also simplify the interpretation of the other kernels in section 3.2 considerably:

- $C(\vec{r}, E' \to E, \hat{\Omega}' \to \hat{\Omega})]$ is the probability density for a particle entering a collision at $\vec{r}$ with energy E' and direction $\hat{\Omega}'$ to have energy and direction $E, \hat{\Omega}$ after the collision;
- $K(P' \to P)$ is the probability density for a particle to go from P' to P by first starting a trajectory from $\vec{r}\,'$ and then colliding at $\vec{r}$ to change its energy and direction;
- $L(P' \to P)$ is the probability density for a particle to go from P' to P by first changing energy and direction in a collision at $\vec{r}\,'$ and starting a flight path to the next collision at $\vec{r}$.

Note that equations (3.7) and (3.8) are a direct result of equations (3.2) and (3.3). Thus, they are equivalent to the neutron transport equation (2.6), provided that the particle mentioned above has the same properties as a neutron. In other words, generating the Markov chain $(P_1, P_0, \ldots)$. comes down to generating the 'life' of a neutron from the time it comes into being till the time it is absorbed or leaks out of the system. Such a 'life' of a particle is called a **history**.

3.4.2 Simulating neutrons

A simulated neutron will start travelling from its initial position in a random direction. In this thesis, only neutrons that scatter *isotropically* are considered. (I.e.: all directions in which the neutron can travel after a collision are equally probable.) In appendix B.3 it is explained how such a direction vector is sampled.

After 'choosing' a direction, the neutron will start its trajectory, after which it will either leak out of the system or enter a collision at some random distance from the initial position. From Eq. (2.3) and appendix B.2, it follows that the distance to the next collision in a homogeneous medium can be sampled by

$$d = -\frac{1}{\Sigma_T}\log(\rho), \tag{3.9}$$

where ρ is uniformly distributed from 0 to 1.

A neutron has no memory. In a medium with a piecewise constant total cross section, the particle can thus be stopped when it enters a different segment. A new random distance can then be sampled in the new segment.

In a medium with a continuously changing total cross section, a method called **hole tracking** can be used. One simply adds a 'dummy reaction' with a continuously changing **woodcock cross section** Σ_{WC}, such that the total cross section is constant. If a particle enters a woodcock collision, it starts a new trajectory with the same energy and direction. Unfortunately, this method is rather inefficient if Σ_T has a great spatial variance, since in that case Σ_{WC}/Σ_T can be far larger than zero.

If a neutron enters a collision, several different types of nuclear reactions can occur. In this thesis, only three will be considered: capture, scattering and fission reactions. The corresponding cross sections are respectively Σ_c, Σ_s and Σ_f, so $\Sigma_T = \Sigma_c + \Sigma_s + \Sigma_f$. For simplicity, all neutrons will be considered to have the same energy, so all scattering is elastic. The probability for a reaction of type $\langle j \rangle$ to occur, conditional on the event that a reaction occurs, is $\Sigma_{\langle j \rangle}/\Sigma_T$.

In the event of absorption (fission or capture), the history ends. In case a scattering reaction is selected, a new direction is sampled and the neutron starts a new path. If a fission reaction occurs, an integer number of new fission neutrons is sampled. The source $S^{(x)}$ consists of all fission neutrons that were generated in cycle x.

In a typical calculation, the number of simulated histories is in the range $10^3 - 10^5$, whilst the total number of cycles has an order of magnitude of $10^2 - 10^4$.

3.5 Criticality calculation using the Monte Carlo method

The criticality k can be estimated using the neutron histories. In principle, this can be done by counting the number of neutrons in a cycle and divide it by the number of neutrons in the previous cycle. The number of neutrons in cycle n

should be about k times as big as the number of neutrons in cycle $n-1$. [1]

$$k = \mathbb{E}\left[\frac{\text{fission neutrons generated in cycle } j+1}{\text{fission neutrons generated in cycle } j}\right] \tag{3.10}$$

However, the number of simulated histories might grow exponentially or die out if several cycles are generated. This will quickly turn into a serious problem when simulating the Markov chain $(S^{(0)}, S^{(1)}, \ldots)$, so a 'trick' has to be applied to ensure that the number of simulated neutrons is more or less the same for every cycle.

To this end, modify Eq. (3.4):

$$\chi(P) = \frac{1}{k'}S(P) + \int K(P' \to P)\chi(P')\ \mathrm{d}P'. \tag{3.11}$$

This means that the number of neutrons that start a flight path at a source is reduced by a factor $(k')^{-1}$. (To achieve this, the average number of new neutrons in a fission reaction is multiplied by $(k')^{-1}$.) If $k' = k$, the number of neutrons that originate from fission sources is constant for every cycle. Eq. (3.11) is therefore an eigenvalue equation. Solving it comprises finding the value for k' for which $\int \chi(P)\ \mathrm{d}P$ is constant for all cycles.

Since this is not a deterministic calculation, the number of neutrons that are generated in a cycle might still be different from the expected number of fission neutrons. To compensate for this, the average number of fission neutrons generated per fission reaction in cycle j is multiplied by $N^\star/N_j$, where N_j is the number of neutrons at the start of the cycle and $N^\star$ is the **nominal** number of neutrons. On average, $N^\star$ histories are generated per cycle.

Summarising, in cycle j the average number of new neutrons simulated in the event of fission should be $\nu^\star = \nu/k'(N^\star/N_j)$, where ν is the (actual, physical) average number of fission neutrons created in the event of fission. In the first cycle, an initial guess of $\nu^* = \nu$ can be used.

Note that the estimator for k from formula (3.10) will no longer work. Fortunately, this is easily solved by multiplying the estimator with $k'(N_j/N^\star)$.

For each cycle the value of k' that is used in Eq. (3.11) is the estimate of k that was calculated with Eq. (3.14) in the previous cycle. In theory, the expectation value of k' will converge to k after some amount of inactive cycles, so the criticality can be estimated as the average value of k' over all the active cycles.

3.6 The scoring method

Several interesting quantities can be calculated by keeping track of how the (simulated) neutrons behave. Specifically, one can keep **scores** during the simulation of the histories. To illustrate this concept, consider the problem of trying to estimate the average flux in a volume.

From equations (2.5) and (2.4), the *total* reaction rate density (corresponding to any collision) is $\Sigma_T\phi$. But this is just equal to the collision density, which can easily be determined using the neutron histories. Simply determine the average

number of times a neutron has a collision in the volume. To determine the flux, note that $\phi = \psi/\Sigma_T$. Now the flux can be approximated with the estimator

$$\hat{\phi} = \frac{1}{N^* V} \sum_i \left(\frac{1}{\Sigma_T} \right)_{c_i}, \tag{3.12}$$

where V is the size of the volume in which the flux is estimated and c_i is the i^{th} collision. This means that each time a neutron enters a collision, a value of $1/\Sigma_T$ is counted.[4]

In general, such a value is called a **tally**, whilst the sum of all tallies is referred to as the **score**. **Tallying** is the process of counting (scoring) the tallies. [1]

Sometimes there are several tallying methods to estimate the same quantity. For example, Sjenitzer ([4], 15-17) derives the following estimator for the average flux on a surface:

$$\hat{\phi} = \frac{1}{N^* A} \sum_j \left(\frac{1}{|\mu|} \right)_j, \tag{3.13}$$

where A is the area of the surface. The summation runs over all crossings j of the surface at an angle μ with the normal vector.

3.7 Standard variance reduction methods

If the variance of the samples in a Monte Carlo calculation is high, an accurate answer can only be achieved by generating a large amount of samples. This can be very costly and make the calculation impractical. Therefore, various variance reducing methods have been developed. They should reduce the time needed to make an accurate guess of the final answer.

In this section some standard variance reducing methods will be discussed. All of these have been incorporated in every calculation in this thesis.

Instead of sampling the reaction type in the event of a collision, the different types of reactions can be made implicit in every collision.

For example, instead of determining whether a fission event took place and sampling the number of fission neutrons from a predetermined distribution, new neutrons are created after *each* collision. The average number of new neutrons after any collision should be equal to $\nu^\star \Sigma_f/\Sigma_T$, since that's the expectation value for the number of fission neutrons, conditional on the event of a collision.

The final result of the Monte Carlo simulation will remain unbiased as long as the average number of new fission neutrons created after a collision is unchanged. Therefore, one can simply sample $\lfloor \nu^\star \Sigma_f/\Sigma_T \rfloor$[5] neutrons with probability $\lfloor \nu^\star \Sigma_f/\Sigma_T \rfloor - \nu^\star + 1$ or $\lfloor \nu^\star \Sigma_f/\Sigma_T \rfloor + 1$ neutrons with probability $\nu^\star - \lfloor \nu\star \Sigma_f/\Sigma_T \rfloor$.

Absorption can also be made implicit by gradually letting a neutron 'die' a little after each collision. To facilitate this, a **weight** factor is introduced. A particle with weight w is considered to be w^{th} of a particle. If it enters a

[4] In general, the cross sections may not be constant in space; it could be that Σ_T is different for each collision.

[5] Here $\lfloor - \rfloor$ is the floor operator.

collision, it will create $w(\nu^\star \Sigma_f/\Sigma_T)$ new neutrons on average after each collision. All tallies should also be multiplied by the weight.

The probability a neutron will end its history conditional on the event of a collision is Σ_a/Σ_T.[6] Thus, instead of sampling the event of absorption, the weight of a neutron is reduced by a factor of $1 - \Sigma_a/\Sigma_T$ every time it leaves a collision. The weight of a neutron that has just been born is usually unity.

Implicit absorption and implicit fission reduce variance, because the neutrons behave more alike. Instead of letting the histories stop abruptly at arbitrary points, weighting allows the particles to be 'smeared out'. Instead of having a few points with lots of fission neutrons, the new neutrons are more evenly distributed.

Along the same line of reasoning, a better estimator for k can be derived. If Σ_f is the cross section for fission reactions, then 'physical' neutrons (not the simulated ones) will create $\nu\Sigma_f/\Sigma_T$ fission neutrons on average in an arbitrary collision. Thus a new estimator for the criticality would be

$$\begin{aligned} \hat{k} &= \frac{\mathbb{E}\left[\text{number of new fission neutrons generated in cycle } j\right]}{\text{neutrons started in cycle } j} \\ &= \frac{1}{N^*} \sum_i \left(\nu\Sigma_f/\Sigma_T\right)_{c_i}. \end{aligned} \tag{3.14}$$

The summation runs over all collisions c_i in cycle j. This is just another example of estimating a quantity with the scoring method. This time the tally is $\nu\Sigma_f/\Sigma_T$. (Again, it might have a different value for every collision.)

A problem with implicit absorption is that it may take a very long time to simulate histories, since they are only stopped once a particle leaks out of the system. Furthermore, a particle with a low weight will not contribute significantly to the final result of the calculation, so it is a waste to spend a lot of calculation time on it.

This can be solved in the following manner. Suppose the weight $w^\star$ of the particle drops below a predetermined limit w_{RR}. It will then undergo **Russian roulette**. The particle has a probability of survival of w_{sur} and a probability $1 - w_{sur}$ of getting **killed** ('**shot**'), in which case the history is ended. If the particle survives, the weight is set to a new value of $w^\star/w_{sur}$. Russian roulette is guaranteed not to introduce a bias, because the expectation value of the new weight of the particle is equal to the old weight:

$$\begin{aligned} &\mathbb{P}\left[\text{survival}\right]\left(\text{weight after survival}\right) + \mathbb{P}\left[\text{getting shot}\right]\left(\text{weight after getting shot}\right) \\ &= \left(w_{sur}\right)\left(w^\star/w_{sur}\right) + \left(1 - w_{sur}\right)0 \quad = w^\star. \end{aligned}$$

A higher value of w_{RR} increases the variance, but reduces the computation time.

3.8 Difficulties

There are still some difficulties in implementing the Monte Carlo method for neutron transport. Some of them are listed here. They will be discussed in more detail in later chapters.

[6] Remember that Σ_a is the absorption cross section, and that it includes both capture and fission.

1. Despite the efforts from the previous section, it may still take a large computational effort to make a reasonably accurate estimate of the desired quantity. This is especially true for estimating quantities in regions where there is a low flux. Few simulated neutrons will travel there, so there will be few tallies and thus a greater uncertainty is involved in estimating the average.

2. A more fundamental problem arises from the fact that the source iteration is performed only once and several sources in the source iteration are used. Since the $\{S^{(m)}, m \geq M\}$ will, in general, be correlated, it is difficult to determine the standard deviation of the estimations of the criticality in the cycles. This makes it impossible to determine the error in the final answer.

3. It is not easy to verify that the source distribution converges at the same time the estimations of k do. Also, the power method does not guarantee that the source distribution will converge to the flux at all if there are local minima.

   Consider a situation where there are two or more regions where fission might occur that are separated by several mean free paths of the neutron and all neutron start in just one of the regions. Physically, if some of the neutrons cross over to another region, they might multiply there. However, if the total number of simulated histories per cycle is kept approximately constant at N^*. Therefore, it may well be that the neutrons that crossed over die out after some cycles, since their total number is kept low.

   Systems like these are called **loosely coupled**. Their most well-known occurrence is in the storage of used-up fuel assemblies, where there is usually some material in between the fuel assemblies.

Chapter 4

The Correcton Method

Some of the difficulties with simulating neutrons (section 3.8) are a result of the shape of the neutron density in a system. The idea of the correcton method is to simulate other particles that have similar properties to neutrons and have the same criticality, but that have a different flux shape.

4.1 Introduction and justification

To introduce the correcton method in the simplest possible framework, the neutron transport Eq. (2.6) can be rewritten in a time-independent, mono-energetic form with isotropic scattering. Define $S(\vec{r})$ as the source term for *all* neutrons that come into being at $\vec{r}$, regardless of their direction or energy. Since S is no longer a function of time, this means that

$$S(\vec{r}) \equiv \int S(\vec{r},\hat{\Omega})\ \mathrm{d}\hat{\Omega} \equiv \int\int S(\vec{r},E,\hat{\Omega})\ \mathrm{d}E\mathrm{d}\hat{\Omega} = \int\int S(\vec{r},E,\hat{\Omega},t)\ \mathrm{d}E\mathrm{d}\hat{\Omega}\ .$$

Because of the fact that everything is considered to be mono-energetic and time-independent, the neutron density can be written as $n(\vec{r},\hat{\Omega})$. In combination with isotropic scattering, this also implies that $\Sigma_s(E'\to E,\hat{\Omega}'\to\hat{\Omega})$ is not a function of E' or E and is constant for all $\hat{\Omega}'$ and $\hat{\Omega}$. Note too that $\frac{\partial n}{\partial t}=0$.

Integrating over energy and direction and recalling the definition of the neutron flux, the neutron transport equation can now be written as

$$\hat{\Omega}\cdot\vec{\nabla}\phi(\vec{r},\hat{\Omega}) + \Sigma_T\phi(\vec{r},\hat{\Omega}) = \frac{\Sigma_s}{4\pi}\int\phi(\vec{r},\hat{\Omega})\ \mathrm{d}\hat{\Omega} + \frac{S(\vec{r})}{4\pi}\ . \tag{4.1}$$

Since there is no external source, the source is just the fission reaction rate and it can be written as $S(\vec{r}) = \int \nu\Sigma_f\phi(\vec{r},\hat{\Omega})\mathrm{d}\hat{\Omega}$. For a criticality calculation, Eq. (4.1) is again transformed to an eigenequation by dividing the number of neutrons that are born by k':

$$\hat{\Omega}\cdot\vec{\nabla}\phi(\vec{r},\hat{\Omega}) + \Sigma_T\phi(\vec{r},\hat{\Omega}) = \frac{\Sigma_s}{4\pi}\int\phi(\vec{r},\hat{\Omega})\ \mathrm{d}\hat{\Omega} + \frac{1}{k'}\frac{\nu\Sigma_f}{4\pi}\int\phi(\vec{r},\hat{\Omega})\mathrm{d}\hat{\Omega}\ , \tag{4.2}$$

so the criticality is the eigenvalue of k'.

The next step is to decompose the scalar neutron flux:

$$\phi(\vec{r},\hat{\Omega}) = \Upsilon(\vec{r})\ \mathcal{C}(\vec{r},\hat{\Omega}), \tag{4.3}$$

where Υ is a function of position only. $\mathcal{C}(\vec{r}, \hat{\Omega})$ can be considered a multiplicative correction of Υ. After some manipulation (ref. [4], 25-26,41), substituting Eq. (4.3) in Eq. (4.2) results in

$$\begin{aligned} &\hat{\Omega} \cdot \vec{\nabla} \mathcal{C}(\vec{r}, \hat{\Omega}) + \left[\Sigma_T + \hat{\Omega} \cdot \vec{\nabla} \ln \Upsilon(\vec{r})\right] \mathcal{C}(\vec{r}, \hat{\Omega}) \\ &= \frac{\Sigma_s}{4\pi} \int \mathcal{C}(\vec{r}, \hat{\Omega}) \, \mathrm{d}\hat{\Omega} + \frac{1}{k'} \frac{\nu\Sigma_f}{4\pi} \int \mathcal{C}(\vec{r}, \hat{\Omega}) \, \mathrm{d}\hat{\Omega} \, . \end{aligned} \tag{4.4}$$

Comparing this to the neutron transport equation (4.2), it is apparent that the only difference is that ϕ is replaced by $\mathcal{C}$ and some value has been added to the total cross section. Note however, that it is still an eigenequation, so the criticality can still be calculated by solving the equation by means of the Markov chain Monte Carlo (MCMC) power method.

Since ϕ can be estimated by simulating particles histories in a Monte Carlo calculation, the same can be done for $\mathcal{C}$. (Although it may seem very abstract physically to simulate self-made particles, mathematically it isn't any stranger then simulating the neutron transport equation with neutrons.)

These new particles are called **correctons**. The only difference with neutrons they have an effective total cross section of

$$\Sigma_T^{\mathrm{c}} = \Sigma_T + \hat{\Omega} \cdot \vec{\nabla} \ln \Upsilon(\vec{r}) \, . \tag{4.5}$$

Because their fission and scattering cross sections are the same as for neutrons, their absorption cross section should be

$$\Sigma_a^{\mathrm{c}} = \Sigma_a + \hat{\Omega} \cdot \vec{\nabla} \ln \Upsilon(\vec{r}) \, .^{1} \tag{4.6}$$

Simulating correctons only requires a minor manipulation of the simulation of neutrons. The only difference is that some of the cross sections depend on the position and direction of the neutron. Therefore, the tallies and the number of new correctons in the event of implicit fission differ from those of neutrons.

From the previous discussion, it is still unclear why the correcton method would provide better results than a regular simulation with neutrons. The main advantage is that correctons can be steared by the choice of Υ.

For a particle that moves towards a greater value of $\hat{\phi}(\vec{r})$, $\hat{\Omega} \cdot \vec{\nabla} \ln \hat{\phi}(\vec{r})$ is positive. This means that the total cross section is greater, so the correcton doesn't travel very far. Conversely, if the particle is moving towards a position where $\hat{\phi}(\vec{r})$ is smaller, $\hat{\Omega} \cdot \vec{\nabla} \ln \hat{\phi}(\vec{r})$ will have a negative value and the correcton will travel a bit further than a neutron would have done.

Sjenitzer [4] used this to do a more efficient calculation of the flux at a large distance from a source, by choosing Υ in such a way that the correctons were directed towards the region of interest. Huisman [8] extended this to three dimensions.

[1] To avoid confusion, Σ_a and Σ_T are still used to denote the cross sections for neutrons. Correcton cross sections will be indicated by the superscript c.

4.2 The choice of $\Upsilon(\vec{r})$

4.2.1 Limitations

Equations (4.5) and (4.6) seem to put some restrictions on the choice of $\Upsilon(\vec{r})$. A negative total cross section not only has no physical interpretation, but (more importantly) it also renders sampling a random distance with Eq. (3.9) impossible. Therefore, Υ must be chosen in such a way that

$$\min\left(\Sigma_T + \hat{\Omega}\cdot\vec{\nabla}\ \ln\ \Upsilon(\vec{r})\right) > 0\ .$$

Recalling that $\left|\hat{\Omega}\right| \equiv 1$, it is obvious that $\arg\min_{\hat{\Omega}}\left(\hat{\Omega}\cdot\vec{\nabla}\ln\Upsilon(\vec{r})\right) = -\frac{\vec{\nabla}\ln\Upsilon(\vec{r})}{\left|\vec{\nabla}\ln\Upsilon(\vec{r})\right|}$ and thus the equation above simplifies to

$$\left|\vec{\nabla}\ln\Upsilon(\vec{r})\right| < \Sigma_T\ \forall\ \vec{r}\ . \tag{4.7}$$

Note that this does not guarantee that $\Sigma_a^c > \Sigma_f$ or even $\Sigma_a^c > 0$. However, it is not so clear whether this is problematic when the method of implicit absorption from section (3.7) is used. A negative absorption cross section leads to an increase in the weight of the particle if it enters a collision. This should not pose a problem, since the effects of absorption are only implicitly present in the second term on the rhs of Eq. (4.4). The production term $(v\Sigma_f/4\pi)\int\mathcal{C}(\vec{r},\hat{\Omega})\ \mathrm{d}\hat{\Omega}$ also remains unaffected if the absorption cross section drops below the fission cross section.

Without mentioning it explicitly, Becker [6], Becker et al. [5] and Huisman [8] have all used negative absorption cross sections without encountering any difficulties.

Since the neutron flux is continuous, Eq. (4.3) implies that discontinuities in $\Upsilon(\vec{r})$ should be compensated by discontinuities in $\mathcal{C}(\vec{r},\hat{\Omega})$. These do not naturally occur in the flux profile of correctons. Therefore, discontinuities will have to be 'artificially' implemented in $\mathcal{C}$. This can easily be done by changing the weight of particles that cross some discontinuity in Υ.

Specifically, if a particle is in the state $(\vec{r},\hat{\Omega})$, then

$$\lim_{\epsilon\downarrow 0}\phi\left(\vec{r}-\epsilon\hat{\Omega},\hat{\Omega}\right) = \lim_{\epsilon\downarrow 0}\phi\left(\vec{r}+\epsilon\hat{\Omega},\hat{\Omega}\right)$$

implies

$$\lim_{\epsilon\downarrow 0}\ \frac{\mathcal{C}\left(\vec{r}+\epsilon\hat{\Omega},\hat{\Omega}\right)}{\mathcal{C}\left(\vec{r}-\epsilon\hat{\Omega},\hat{\Omega}\right)} = \lim_{\epsilon\downarrow 0}\ \frac{\Upsilon\left(\vec{r}-\epsilon\hat{\Omega},\hat{\Omega}\right)}{\Upsilon\left(\vec{r}+\epsilon\hat{\Omega},\hat{\Omega}\right)} \tag{4.8}$$

and thus the weight of a correcton has to be multiplied by $\lim_{\epsilon\downarrow 0}\ \frac{\Upsilon\left(\vec{r}-\epsilon\hat{\Omega},\hat{\Omega}\right)}{\Upsilon\left(\vec{r}+\epsilon\hat{\Omega},\hat{\Omega}\right)}$ when crossing a discontinuity in Υ.

Note that this is invalid if $\Upsilon = 0$, but equation (4.3) rules out this choice anyway.

4.2.2 Mathematical representation

In this thesis, the systems under consideration are rectangular parallelepipeds that are subdivided by smaller cells that are also rectangular parallelepipeds. The material properties are homogeneous within the cells. $\Upsilon(\vec{r})$ is chosen to be piecewise continuous, that is, it is continuous within the cells.

Let $\hat{x}$, $\hat{y}$ and $\hat{z}$ be cartesian coordinates, so that $\vec{r} = [x, y, z]^T$. The index of a cell is denoted by (i, j, k), meaning that it is the i^{th} cell in the x-direction, the j^{th} cell in the y-direction and the k^{th} cell in the z-direction. Let $\vec{O}_{i,j,k}$ be the centre of the cell.

To avoid the necessity of using hole tracking, the cross sections have to be constant for particles travelling through a cell. If $\Upsilon_{i,j,k}(\vec{r})$ is the function describing $\Upsilon(\vec{r})$ in cell (i, j, k), it must be of the form

$$\begin{aligned} & \vec{\nabla} \ln \Upsilon_{i,j,k}(\vec{r}) && = \text{constant} \\ \Rightarrow \quad & \ln \Upsilon_{i,j,k}(\vec{r}) && = \vec{\beta}_{i,j,k} \cdot \vec{r} + \left(\ln(K_{i,j,k}) - \vec{\beta}_{i,j,k} \cdot \vec{O}_{i,j,k} \right) \\ \Rightarrow \quad & \Upsilon_{i,j,k}(\vec{r}) && = K_{i,j,k} \exp\left[\vec{\beta}_{i,j,k} \cdot \left(\vec{r} - \vec{O}_{i,j,k} \right) \right] , \end{aligned} \tag{4.9}$$

for some parameters $\vec{\beta}_{i,j,k}$ and $K_{i,j,k}$.

Eq. (4.7) now takes on the particularly simple form

$$\left| \vec{\beta}_{i,j,k} \right| < (\Sigma_T)_{i,j,k} , \tag{4.10}$$

where $(\Sigma_T)_{i,j,k}$ is the total cross section in cell (i, j, k). Eq. (4.9) with $|\vec{\beta}_{i,j,k}| \to (\Sigma_T)_{i,j,k}$ is also the function that maximises the slope of $\Upsilon(\vec{r})$ constraint by (4.7). For some given total cross section Σ_T in a material without fission, the neutron flux has a maximum slope if $\Sigma_T = \Sigma_a$, in which case the flux will decrease exponentially and it can only just be described by Eq. (4.9).

4.3 Real time flux estimation

Suppose that $\Upsilon(\vec{r})$ is a reasonably good estimate $\hat{\phi}(\vec{r})$ of the scalar neutron flux $\phi(\vec{r}) \equiv \int \phi(\vec{r}, \Omega)\, \mathrm{d}\Omega$, meaning that it has more or less the same shape:

$$\hat{\phi}(\vec{r}) \propto \phi(\vec{r}) .$$

According to Eq. (4.3), the correcton flux $\mathcal{C}$ should be roughly constant. This may enhance the convergence of the correcton flux distribution, since the correctons do not have a tendency to pile up in some region.

The flux guess may be obtained from a cheap Monte Carlo calculation or a deterministic calculation. To enhance the source convergence, it might even suffice if the flux distribution is only qualitatively correct.

In this thesis, a **real time flux estimation** is proposed. The idea is to tally the flux of the correctons during every cycle and use the results to make better and better estimations of the neutron flux. These new estimations can then be used to adjust $\Upsilon(\vec{r})$ to make it a better representation of the neutron flux.

The two main difficulties are

- determining a $\hat{\phi}(\vec{r})$ from a simulation with correctons;
- adjusting the flux parameters $K_{i,j,k}$ and $\vec{\beta}_{i,j,k}$ to make $\Upsilon(\vec{r})$ as close as possible to the actual flux shape.

These are dealt with in sections 4.4 and 4.5 respectively.

Note that Υ is, in general, different for every cycle. Therefore, the particles have to converge to a different flux distribution in every cycle. To solve this problem, the weights of the particles at the beginning of their history can be adjusted in order change the flux distribution they represent.

Specifically, if Υ_i is used to perform the calculations in cycle i and $\mathcal{C}_i = \phi/\Upsilon_i$, then the correcton flux in cycle j is a multiple of what it was in cycle $j-1$:

$$\frac{\mathcal{C}_j(\vec{r},\Omega)}{\mathcal{C}_{j-1}(\vec{r},\Omega)} = \frac{\phi(\vec{r},\Omega)/\Upsilon_j(\vec{r})}{\phi(\vec{r},\Omega)/\Upsilon_{j-1}(\vec{r})} = \frac{\Upsilon_{j-1}(\vec{r})}{\Upsilon_j(\vec{r})} \tag{4.11}$$

Thus, the weight of a particle at $\vec{r}$ at the beginning of its history in cycle j must be set to $\frac{\Upsilon_{j-1}(\vec{r})}{\Upsilon_j(\vec{r})}$.

4.4 Estimating the neutron flux from correcton histories

The correcton flux can be obtained by tracking the positions of the correctons. The neutron flux equals Υ multiplied by the correcton flux. Therefore, the neutron flux can be found by counting every correcton at $\vec{r}$ as $\Upsilon(\vec{r})$ particles.

Therefore, one can simply tally the neutron flux by using Eq. (3.12) or Eq. (3.13) and multiplying every tally at $\vec{r}$ with $\Upsilon(\vec{r})$.

In this thesis, in every calculation the neutron surface flux was estimated. Compared to using average fluxes, this makes it easier to adjust the parameters of $\Upsilon(\vec{r})$ to the neutron flux shape if $\Upsilon(\vec{r})$ is given by Eq. (4.9).

Suppose a correcton travelling in a direction $\hat{\Omega}$ has a weight w before it crosses from one cell to another at $\vec{r}$. Before it crossed the cell boundary, it was counted as $w \lim_{\epsilon\downarrow 0} \Upsilon(\vec{r} - \epsilon\hat{\Omega})$ neutrons. Since the correcton changes it weight, it is still counted as $\left(w \frac{\lim_{\epsilon\downarrow 0} \Upsilon(\vec{r}-\epsilon\hat{\Omega})}{\lim_{\epsilon\downarrow 0} \Upsilon(\vec{r}+\epsilon\hat{\Omega})}\right) \lim_{\epsilon\downarrow 0} \Upsilon(\vec{r} + \epsilon\hat{\Omega}) = w \lim_{\epsilon\downarrow 0} \Upsilon(\vec{r} - \epsilon\hat{\Omega})$ neutrons after crossing the cell. (This is hardly surprising, since the neutron flux is a continuous quantity.)

It seems best not to change the $\Upsilon_{i,j,k}$ in every cycle, but instead to let the tallies accumulate over several cycles and only then to determine a new flux estimate. There are two principle reasons for this. First, it is possible that not all boundaries have been crossed by a particle after just one cycle. This means that the estimate of the average correcton flux over some of the boundaries might be zero, in which case none of the analyses in section 4.5 makes sense.

Secondly, there will be less statistical variation in the surface flux estimates. Therefore, one would expect to see fewer cases where adjacent cells have a large discontinuity in $\Upsilon(\vec{r})$.

To ensure that the tallies in every cycle have approximately the same amount of influence on the final estimate of the neutron flux, the sum of the flux estimates over all boundaries should be normalised in every cycle.

4.5 Estimating the flux parameters

Every cell has six boundaries, whilst there are only four degrees of freedom in the parameters $\vec{\beta}_{i,j,k}$ and $K_{i,j,k}$. In general, it is therefore impossible to satisfy all boundary conditions. However, the correcton flux can still be made flatter, and thus more stable, if only Υ has more or less the same shape as the neutron flux.

Since $\vec{\nabla} \ln \Upsilon_{i,j,k}(\vec{r})$ depends solely on the $\vec{\beta}_{i,j,k}$, the $K_{i,j,k}$ do not influence the cross sections of the particles. However, the weight change of the particle *is* effected by the choice of the $K_{i,j,k}$ via Eq. (4.8).

If the weight multiplication is very large, some particles will have very high weights. Big differences between the weights of the particles lead not only to a higher variance in the calculation, but can also result in large concentrations of new fission particles, which can destabilise the calculation.

Therefore, the task at hand is to choose the $\vec{\beta}_{i,j,k}$ such that the correctons are driven towards regions with a low neutron flux, whilst the $K_{i,j,k}$ should be adjusted to make the weight changes of the particles crossing cells borders are as small as possible. Unfortunately, this is far from trivial.

4.5.1 Choosing $\vec{\beta}_{i,j,k}$

Suppose the lengths of the ribs of cell (i,j,k) in the x-, y- and z-direction are $2A_{i,j,k}$, $2B_{i,j,k}$ and $2C_{i,j,k}$ respectively. The estimated average neutron fluxes at the boundaries of the cell are presumed to be known and equal $\mathcal{F}_{i^{\pm},j,k}$, $\mathcal{F}_{i,j^{\pm},k}$ and $\mathcal{F}_{i,j,k^{\pm}}$ for the boundaries $\vec{r}\cdot\hat{x} = \vec{O}_{i,j,k}\cdot\hat{x} \pm A_{i,j,k}$, $\vec{r}\cdot\hat{y} = \vec{O}_{i,j,k}\cdot\hat{y} \pm B_{i,j,k}$ and $\vec{r}\cdot\hat{z} = \vec{O}_{i,j,k}\cdot\hat{z} \pm C_{i,j,k}$ respectively.[2]

One might choose the $\vec{\beta}_{i,j,k}$ such that the multiplicative error between Υ and and the neutron flux is equal for opposing boundaries, i.e.:

$$\begin{aligned}
\frac{\Upsilon(\vec{O}_{i,j,k}\cdot\hat{x} + A_{i,j,k}, y, z)}{\mathcal{F}_{i^+,j,k}} &= \frac{\Upsilon(\vec{O}_{i,j,k}\cdot\hat{x} - A_{i,j,k}, y, z)}{\mathcal{F}_{i^-,j,k}} \\
\frac{\Upsilon(x, \vec{O}_{i,j,k}\cdot\hat{y} + B_{i,j,k}, z)}{\mathcal{F}_{i,j^+,k}} &= \frac{\Upsilon(x, \vec{O}_{i,j,k}\cdot\hat{y} - B_{i,j,k}, z)}{\mathcal{F}_{i,j^-,k}} \\
\frac{\Upsilon(x, y, \vec{O}_{i,j,k}\cdot\hat{z} + C_{i,j,k})}{\mathcal{F}_{i,j,k^+}} &= \frac{\Upsilon(x, y, \vec{O}_{i,j,k}\cdot\hat{z} - C_{i,j,k})}{\mathcal{F}_{i,j,k^-}} \,.
\end{aligned}$$

This leads to

$$\vec{\beta}_{i,j,k} = \left[\frac{1}{2A_{i,j,k}}\ln\left(\frac{\mathcal{F}_{i^+,j,k}}{\mathcal{F}_{i^-,j,k}}\right), \frac{1}{2B_{i,j,k}}\ln\left(\frac{\mathcal{F}_{i,j^+,k}}{\mathcal{F}_{i,j^-,k}}\right), \frac{1}{2C_{i,j,k}}\ln\left(\frac{\mathcal{F}_{i,j,k^+}}{\mathcal{F}_{i,j,k^-}}\right)\right]^T , \tag{4.12}$$

regardless of $K_{i,j,k}$. However, this does not guarantee that the restriction (4.10) is met, so an adjustment is necessary. In an effort to maintain the shape of Υ as much as possible, one may choose to multiply the $\vec{\beta}_{i,j,k}$ with a factor that

[2] This isn't a particularly elegant notation, since the same neutron flux can sometimes be denoted in two different manners. (For example $\mathcal{F}_{2^-,j,k} \equiv \mathcal{F}_{1^+,j,k}$.) However, it is easy to use.

makes them satisfy Eq. (4.10):

$$\vec{\beta}_{i,j,k} = \min\left(\frac{(\Sigma_T)_{i,j,k}}{\ell_{i,j,k}}, 1\right)\left[\frac{\ln\left(\frac{\mathcal{F}_{i^+,j,k}}{\mathcal{F}_{i^-,j,k}}\right)}{2A_{i,j,k}}, \frac{\ln\left(\frac{\mathcal{F}_{i,j^+,k}}{\mathcal{F}_{i,j^-,k}}\right)}{2B_{i,j,k}}, \frac{\ln\left(\frac{\mathcal{F}_{i,j,k^+}}{\mathcal{F}_{i,j,k^-}}\right)}{2C_{i,j,k}}\right]^T, \tag{4.13}$$

where, for convenience, the definition

$$\ell_{i,j,k} \equiv \sqrt{\left(\frac{\ln\left(\frac{\mathcal{F}_{i^+,j,k}}{\mathcal{F}_{i^-,j,k}}\right)}{2A_{i,j,k}}\right)^2 + \left(\frac{\ln\left(\frac{\mathcal{F}_{i,j^+,k}}{\mathcal{F}_{i,j^-,k}}\right)}{2B_{i,j,k}}\right)^2 + \left(\frac{\ln\left(\frac{\mathcal{F}_{i,j,k^+}}{\mathcal{F}_{i,j,k^-}}\right)}{2C_{i,j,k}}\right)^2}$$

has been used.

Note that the $\mathcal{F}_{i^\pm,j^\pm,k^\pm}$ are usually different from one another, so none of the cartesian components of $\vec{\beta}_{i,j,k}$ are zero. So long as $\vec{\beta}_{i,j,k} \neq \vec{0}$, the following analyses in this chapter is not fundamentaly changed, although some mathematical results are slightly different.

4.5.2 Adjusting the $K_{i,j,k}$

The $K_{i,j,k}$ should be chosen such that the excesses of the weights of the particles are controlled, so a quantity of interest is the maximal multiplicative weight change for a particle crossing from cell (a, b, c) to cell (d, e, f), denoted by $m(a, b, c \to d, e, f)$. One would like to find the $K_{i,j,k}$ by solving

$$K_{i,j,k} = \arg\min_{K_{i,j,k}}\left[\max_{a,b,c,d,e,f}\{m(a,b,c \to e,d,f)\}\right]. \tag{4.14}$$

Suppose a particle crosses from, say, cell (i, j, k) to cell $(i + 1, j, k)$ at $Y \equiv \left(\vec{r} - \vec{O}_{i,j,k}\right)\cdot\hat{y} = \left(\vec{r} - \vec{O}_{i+1,j,k}\right)\cdot\hat{y}$ and $Z \equiv \left(\vec{r} - \vec{O}_{i,j,k}\right)\cdot\hat{z} = \left(\vec{r} - \vec{O}_{i+1,j,k}\right)\cdot\hat{z}$. That is, the distance between the particle and the centres of the cells is Y in the $\hat{y}$-direction and Z in the $\hat{z}$-direction. The weight is changed by a factor

$$\frac{K_{i,j,k}}{K_{i+1,j,k}}\exp\left[+\left(\vec{\beta}_{i,j,k}\cdot\hat{x}\right)A_{i,j,k} + \left(\vec{\beta}_{i+1,j,k}\cdot\hat{x}\right)A_{i+1,j,k}\right.$$
$$\left.+Y\left(\vec{\beta}_{i,j,k}\cdot-\vec{\beta}_{i+1,j,k}\right)\cdot\hat{y} + Z\left(\vec{\beta}_{i,j,k}\cdot-\vec{\beta}_{i+1,j,k}\right)\cdot\hat{z}\right]. \tag{4.15}$$

Using Eq. (4.15) with $|Y| \leq B_{i,j,k}$ and $|Z| \leq C_{i,j,k}$,

$$m(i,j,k \to i+1,j,k) = \frac{K_{i,j,k}}{K_{i+1,j,k}}\exp\left[+\left(\vec{\beta}_{i,j,k}\cdot\hat{x}\right)A_{i,j,k} + \left(\vec{\beta}_{i+1,j,k}\cdot\hat{x}\right)A_{i+1,j,k}\right.$$
$$\left.+B_{i,j,k}\left|\left(\vec{\beta}_{i,j,k} - \vec{\beta}_{i+1,j,k}\right)\cdot\hat{y}\right| + C_{i,j,k}\left|\left(\vec{\beta}_{i,j,k} - \vec{\beta}_{i+1,j,k}\right)\cdot\hat{z}\right|\right]. \tag{4.16}$$

Similarly, the maximal multiplicative weight change of a particle crossing the same border in the other direction is

$$m(i+1,j,k \to i,j,k) = \frac{K_{i+1,j,k}}{K_{i,j,k}} \exp\Bigg[-\left(\vec{\beta}_{i,j,k}\cdot\hat{x}\right) A_{i,j,k} - \left(\vec{\beta}_{i+1,j,k}\cdot\hat{x}\right) A_{i+1,j,k} \\ + B_{i,j,k}\left|\left(\vec{\beta}_{i+1,j,k}-\vec{\beta}_{i,j,k}\right)\cdot\hat{y}\right| + C_{i,j,k}\left|\left(\vec{\beta}_{i+1,j,k}-\vec{\beta}_{i,j,k}\right)\cdot\hat{z}\right|\Bigg] . \tag{4.17}$$

Therefore, minimising the maximum relative weight change of particles crossing the boundary between cell (i,j,k) and cell $(i+1,j,k)$ in any direction comprises minimising

$$\max\left[\frac{K_{i+1,j,k}/K_{i,j,k}}{\exp\left[\left(A_{i,j,k}\vec{\beta}_{i,j,k}+A_{i+1,j,k}\vec{\beta}_{i+1,j,k}\right)\cdot\hat{x}\right]}, \frac{\exp\left[\left(A_{i,j,k}\vec{\beta}_{i,j,k}+A_{i+1,j,k}\vec{\beta}_{i+1,j,k}\right)\cdot\hat{x}\right]}{K_{i+1,j,k}/K_{i,j,k}}\right],$$

which leads to

$$\frac{K_{i+1,j,k}}{K_{i,j,k}} = \exp\left[\left(A_{i,j,k}\vec{\beta}_{i,j,k}+A_{i+1,j,k}\vec{\beta}_{i+1,j,k}\right)\cdot\hat{x}\right] . \tag{4.18}$$

Thus, if all $\vec{\beta}_{i,j,k}$ are (anti)parallel to $\hat{x}$, then the solution to Eq. (4.14) should satisfy Eq. (4.18). (The results are similar for particles crossing from one cell to another in the y- or z-direction.)

Unfortunately, finding a closed-form solution to Eq. (4.14) is very difficult for the general case. (In fact, it may well be impossible.)

Applying some physical insight, it seems reasonable that the estimate of the average neutron flux at the boundaries of a cell should be equal to the average value of Υ at the boundaries. $K_{i,j,k}$ can then be adjusted to ensure that

$$\iint_{\text{all 6 surfaces}} \Upsilon(x,y,z)\,\mathrm{d}\mathcal{Y} = \left(F_{i^+,j,k}+F_{i,j^+,k}+F_{i,j,k^+}+F_{i^-,j,k}+F_{i,j^-,k}+F_{i,j,k^-}\right) \tag{4.19}$$

The 'x-boundaries' of cell (i,j,k) (i.e.: the boundaries with normal vectors that are (anti)parallel to $\hat{x}$) are given by $\left(\vec{r}-\vec{O}_{i,j,k}\right)\cdot\hat{x} = \pm A_{i,j,k}$ and thus the integrals of Υ over those surfaces are

$$\int_{z=\vec{O}_{i,j,k}\cdot\hat{z}-C_{i,j,k}}^{\vec{O}_{i,j,k}\cdot\hat{z}+C_{i,j,k}} \int_{y=\vec{O}_{i,j,k}\cdot\hat{y}-B_{i,j,k}}^{\vec{O}_{i,j,k}\cdot\hat{y}+B_{i,j,k}} \mathrm{d}y\ \mathrm{d}z\ \Upsilon_{i,j,k}(\vec{O}_{i,j,k}\cdot\hat{x}\pm A_{i,j,k}\ ,y,z) \\ = \frac{K_{i,j,k}\left(\mathrm{e}^{B_{i,j,k}\left(\vec{\beta}_{i,j,k}\cdot\hat{y}\right)}-\mathrm{e}^{-B_{i,j,k}\left(\vec{\beta}_{i,j,k}\cdot\hat{y}\right)}\right)\left(\mathrm{e}^{C_{i,j,k}\left(\vec{\beta}_{i,j,k}\cdot\hat{z}\right)}-\mathrm{e}^{-C_{i,j,k}\left(\vec{\beta}_{i,j,k}\cdot\hat{z}\right)}\right)}{\mathrm{e}^{\mp A_{i,j,k}\left(\vec{\beta}_{i,j,k}\cdot\hat{x}\right)}\left(\vec{\beta}_{i,j,k}\cdot\hat{y}\right)\left(\vec{\beta}_{i,j,k}\cdot\hat{z}\right)} \tag{4.20}$$

with similar expressions for the other boundaries of the cell. The integral of

$\Upsilon(\vec{r})$ over the total surface $\mathcal{Y}$ of the cell is thus

$$\begin{aligned}
&\iint\limits_{\text{all 6 surfaces}} \Upsilon(x,y,z)\ \mathrm{d}\mathcal{Y} \\
= \quad & \kappa\ K_{i,j,k} \\
& \cdot \Bigg[\left(\vec{\beta}_{i,j,k}\cdot\hat{x}\right) \frac{\mathrm{e}^{A_{i,j,k}\left(\vec{\beta}_{i,j,k}\cdot\hat{x}\right)} + \mathrm{e}^{-A_{i,j,k}\left(\vec{\beta}_{i,j,k}\cdot\hat{x}\right)}}{\mathrm{e}^{A_{i,j,k}\left(\vec{\beta}_{i,j,k}\cdot\hat{x}\right)} - \mathrm{e}^{-A_{i,j,k}\left(\vec{\beta}_{i,j,k}\cdot\hat{x}\right)}} \\
& + \left(\vec{\beta}_{i,j,k}\cdot\hat{y}\right) \frac{\mathrm{e}^{B_{i,j,k}\left(\vec{\beta}_{i,j,k}\cdot\hat{y}\right)} + \mathrm{e}^{-B_{i,j,k}\left(\vec{\beta}_{i,j,k}\cdot\hat{y}\right)}}{\mathrm{e}^{B_{i,j,k}\left(\vec{\beta}_{i,j,k}\cdot\hat{y}\right)} - \mathrm{e}^{-B_{i,j,k}\left(\vec{\beta}_{i,j,k}\cdot\hat{y}\right)}} \\
& + \left(\vec{\beta}_{i,j,k}\cdot\hat{z}\right) \frac{\mathrm{e}^{C_{i,j,k}\left(\vec{\beta}_{i,j,k}\cdot\hat{z}\right)} + \mathrm{e}^{-C_{i,j,k}\left(\vec{\beta}_{i,j,k}\cdot\hat{z}\right)}}{\mathrm{e}^{C_{i,j,k}\left(\vec{\beta}_{i,j,k}\cdot\hat{z}\right)} - \mathrm{e}^{-C_{i,j,k}\left(\vec{\beta}_{i,j,k}\cdot\hat{z}\right)}} \Bigg] ,
\end{aligned} \tag{4.21}$$

where

$$\begin{aligned}
\kappa \quad \equiv \quad & \left(\mathrm{e}^{A_{i,j,k}\left(\vec{\beta}_{i,j,k}\cdot\hat{x}\right)} - \mathrm{e}^{-A_{i,j,k}\left(\vec{\beta}_{i,j,k}\cdot\hat{x}\right)}\right) \\
& \cdot \left(\mathrm{e}^{B_{i,j,k}\left(\vec{\beta}_{i,j,k}\cdot\hat{y}\right)} - \mathrm{e}^{-B_{i,j,k}\left(\vec{\beta}_{i,j,k}\cdot\hat{y}\right)}\right) \left(\mathrm{e}^{C_{i,j,k}\left(\vec{\beta}_{i,j,k}\cdot\hat{z}\right)} - \mathrm{e}^{-C_{i,j,k}\left(\vec{\beta}_{i,j,k}\cdot\hat{z}\right)}\right) \\
& \cdot \left(\vec{\beta}_{i,j,k}\cdot\hat{x}\right)^{-1} \left(\vec{\beta}_{i,j,k}\cdot\hat{y}\right)^{-1} \left(\vec{\beta}_{i,j,k}\cdot\hat{z}\right)^{-1} .
\end{aligned} \tag{4.22}$$

For some given $\vec{\beta}_{i,j,k}$, Eq. (4.19) is solved for $K_{i,j,k}$ by setting the rhs of 4.19 equal to the rhs of 4.21.

Chapter 5

Numerical Examples

In this chapter, several statements that have been made throughout the previous two chapters are put to the test. Criticality calculations have been performed for different systems. The neutrons are considered to be mono-energetic and there are no delayed neutrons. This makes the systems wildly unrealistic from a physical point of view, but they serve to illustrate some of the points made in the text.

First the theory from the previous chapters is put to the test for a simple homogeneous rectangular parallelepiped, called system 1. Several simulations should convince the reader of the robustness of the proposed correcton method.

Then, a more complicated system of loosely coupled fuel assemblies, called system 2, is studied. It is shown how a conventional neutron calculation fails, while the correcton method provides significantly better results.

Complete specifications of both systems can be found in appendix C.

In every calculation, all variance reducing techniques developed in section 3.7 have been used (including implicit fission and absorption, Russian roulette and the criticality tally (3.14)). The parameters for Russian roulette are always $w_{RR} = 0.1$ and $w_{sur} = 0.5$.

The total number of cycles is always denoted by $\mathcal{M}$; the nominal number of histories per cycle is N^*.

5.1 System 1: a homogeneous rectangular parallelepiped

5.1.1 Basic criticality calculation with neutrons

A basic criticality calculation with neutrons has been performed for system 1. The number of cycles was $\mathcal{M} = 10^5$ and the average number of simulated histories per cycle was $N^* = 10^6$.

Fig. 5.1 shows a typical realisation of the simulation. From the plot, it can be seen how the criticality estimates converge to some value that is close to 1. In the first cycles the neutrons are still more or less uniformly distributed. After the source converges, the particles are more concentrated in the centre

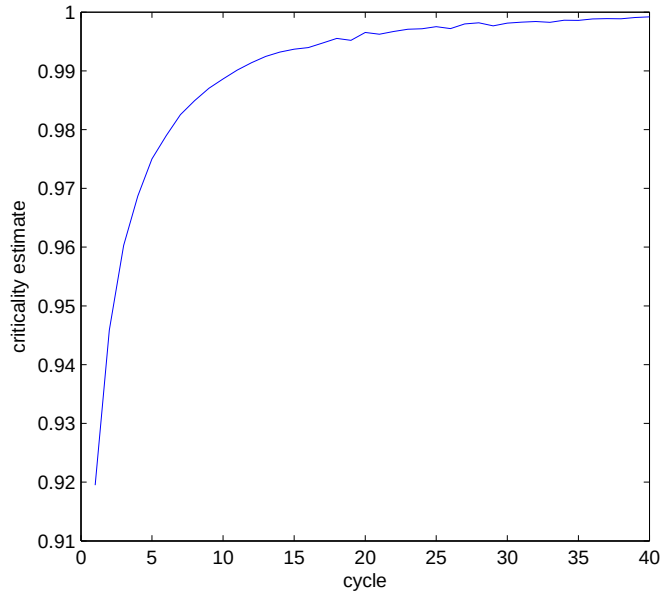

Figure 5.1: criticality estimates during first cycles of neutron calculation for a homogeneous rectangular parallelepiped (system 1)

of the rectangular parallelepiped, so less particles will leak out of the system. Therefore, the criticality estimates are lower in the inactive cycles.

Suppose the first $I = 100$ cycles are taken to be the inactive cycles and the values of the criticality are considered to be i.i.d. This results in a criticality estimate of $k = 1.00013526$ with a standard deviation of $7.7 \cdot 10^{-7}$.

5.1.1.1 Estimating the error of the final result

Fig. 5.2 shows the values of the criticality estimates during some of the active cycles. Even with a Savitzky-Golay filter[1] of order 10000, the estimates for the criticality as a function of the cycle show a clear trending behaviour. In other words, they are far from i.i.d. The positions of the particles in a cycle are strongly positively correlated with the positions of the particles in the previous cycles. Therefore, the estimates of k are positively correlated as well. This renders it very difficult to estimate the error of such a calculation.

The same calculation with $\mathcal{M} = 10^3$ and $N^* = 10^6$ has been performed 33 times with 100 inactive cycles each time. This way, different final values of the criticality were found. From this, it was determined that the standard deviation of the final answer of a single calculation is $1.4 \cdot 10^{-5}$. If, however, the criticality estimates in the active cycles of a single calculation are considered to be i.i.d., the standard deviation in the final answer is estimated to be $(8.1 \pm 0.2) \cdot 10^{-6}$,

[1] A Savitzky-Golay filter of order j is a generalised moving average filter, where the weight coefficients are determined by a polynomial regression of order j. It should smooth a set of data, but compared to a moving average filter it preserves trending behaviour and local extrema better. (Orfanidis, S.J., *Introduction to Signal Processing*, Prentice-Hall, 1996)

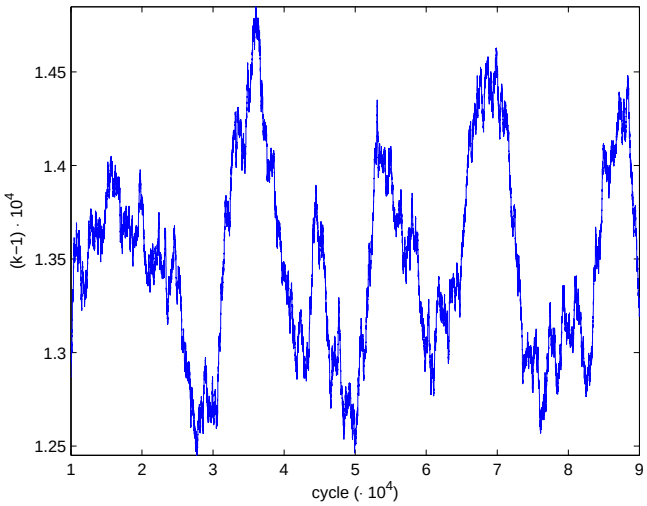

Figure 5.2: criticality estimates k during active cycles of neutron calculation for a homogeneous rectangular parallelepiped (system 1) (smoothed with Savitzky-Golay filter of order 10^4)

which is 1.7 times lower.

In the following sections, the reported error is always based on the standard deviation of the estimates of the criticality. The previous discussion suggests that it should be of the same order of magnitude as the actual error. However, due to positive correlation between the cycles, the true error is most likely larger.

5.1.2 Robustness tests for the correcton method

In this section, several extreme examples are used to test the robustness of the correcton method.

In every case, the neutron flux tallies have been compared to the flux tallies that were obtained from a calculation with neutrons. The results were all indistinguishable. (The neutron flux in the x-, y- or z-direction have a typical cosine shape. This is a well-known result from analytical deterministic methods. ([2], 209))

5.1.2.1 Criticality calculation with correctons for system 1

To facilitate a calculation with correctons, system 1 has been subdivided in two cells: $(1,1,1)$ and $(2,1,1)$. They are separated by the plane $x = 5$ cm.

Two different simulations have been done with $\mathcal{M} = 18500$ and $N^* = 10^6$ each. In the first case, $\vec{\beta}_{1,1,1} = (\Sigma_T)\,\hat{x}$ and $\vec{\beta}_{2,1,1} = \vec{0}$. In the second calculation, $\vec{\beta}_{1,1,1} = -(\Sigma_T)\,\hat{x}$ and $\vec{\beta}_{2,1,1} = \vec{0}$. In both cases, the $K_{i,j,k}$ have been calculated with Eq. (4.18). In this particular case, the $K_{i,j,k}$ can be chosen in such a way that there is no discontinuity in $\Upsilon(\vec{r})$.

Plots of the criticality estimates can be found in figures 5.3 and 5.4. In both cases, the criticality converges to the same value as in section 5.1.1. The

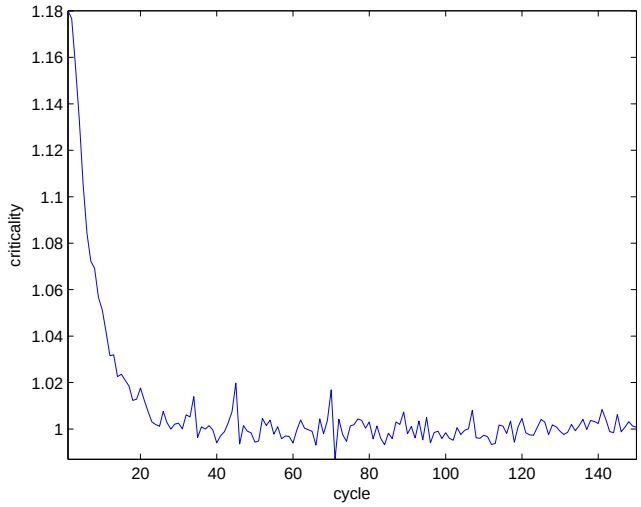

Figure 5.3: criticality estimates during inactive cycles of correcton calculation for a homogeneous rectangular parallelepiped (system 1); $\vec{\beta}_{1,1,1} = (\Sigma_T)\,\hat{x}$ and $\vec{\beta}_{2,1,1} = \vec{0}$

number of inactive cycles is taken to be 50 in each. The estimates are $k = 1.000154 \pm 3.4 \cdot 10^{-5}$ and $k = 1.000121 \pm 1.3 \cdot 10^{-5}$ respectively.

Figures 5.5 and 5.6 show the source distribution of the correctons for $\vec{\beta}_{1,1,1} = (\Sigma_T)\,\hat{x}$ and $\vec{\beta}_{1,1,1} = -(\Sigma_T)\,\hat{x}$ respectively. These plots have been obtained by randomly selecting 1500 particles after each cycle and storing their positions at the beginning of their history. The y-axis indicates the number of times a particle was found in a certain region during any of the active cycles. (Note that only the relative frequencies with which the particles are in certain positions bear any real meaning.)

Since the fission cross section is constant in the medium, and since there is no external source, the source distribution is proportional to the correcton flux $\mathcal{C}$. According to Eq. (4.3), $\mathcal{C}$ should be small in regions where $\Upsilon(\vec{r})$ is very large and vice versa. This is reflected in figures 5.5 and 5.6.

This calculation also confirms that there is no problem with negative absorption cross sections for correctons.

5.1.2.2 Correctons with a discontinuous $\Upsilon(\vec{r})$ in system 1

In the previous calculations, the values for $\vec{\beta}_{i,j,k}$ and $K_{i,j,k}$ were chosen in such a way that that was no discontinuity in $\Upsilon(\vec{r})$. To test the validity of changing the particle weights via Eq. (4.8), a calculation with a discontinuous $\Upsilon(\vec{r})$ has also been performed.

The medium in system 1 is subdivided in 24 cells $(1,1,1), \ldots, (1,1,24)$ that are separated by the planes $z = 1$ cm, 2 cm, $\ldots, z = 23$ cm. The parameters are $\vec{\beta}_{1,1,k} = \vec{0}\ \forall\ k = 1, \ldots, 24$ (so $\Upsilon_{1,1,k}(\vec{r}) = K_{1,1,k}$), whilst the $K_{1,1,k}$ have been randomly chosen from a uniform distribution from 1 to 11. $\mathcal{M} = 1.8 \cdot 10^4$ and

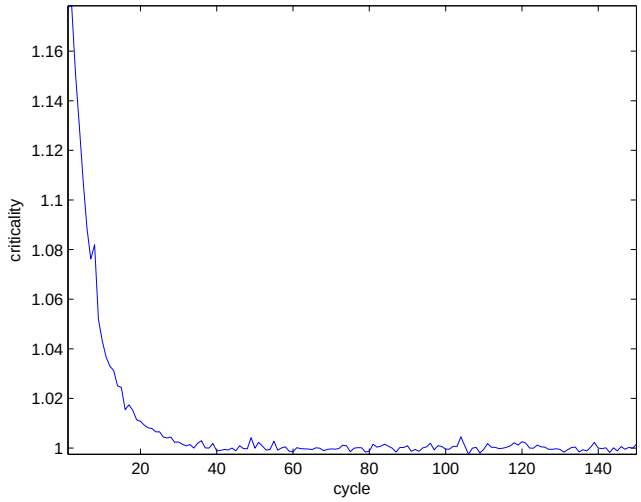

Figure 5.4: criticality estimates during inactive cycles of correcton calculation for a homogeneous rectangular parallelepiped (system 1); $\vec{\beta}_{1,1,1} = -(\Sigma_T)\,\hat{x}$ and $\vec{\beta}_{2,1,1} = \vec{0}$

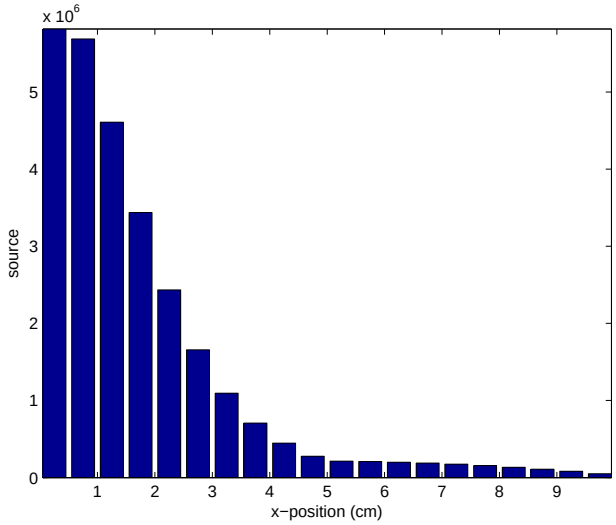

Figure 5.5: source distribution during active cycles of correcton calculation for a homogeneous rectangular parallelepiped (system 1); $\vec{\beta}_{1,1,1} = (\Sigma_T)\,\hat{x}$ and $\vec{\beta}_{2,1,1} = \vec{0}$

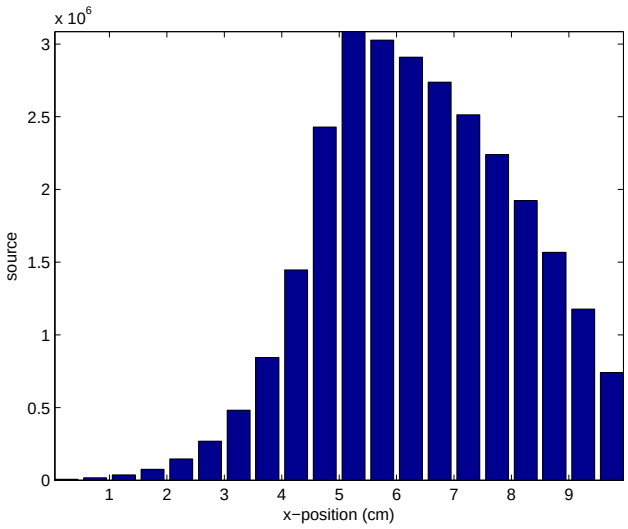

Figure 5.6: source distribution during active cycles of correcton calculation for a homogeneous rectangular parallelepiped (system 1); $\vec{\beta}_{1,1,1} = -(\Sigma_T)\,\hat{x}$ and $\vec{\beta}_{2,1,1} = \vec{0}$

$N^* = 10^6$.

The source distribution has been obtained in the same manner as in figures 5.5 and 5.6. The result is shown in Fig. 5.7.

The initial criticality estimates are displayed in Fig. 5.8. If there are 100 inactive cycles, the criticality is estimated to be $k = 1.0001325 \pm 3.5 \cdot 10^{-6}$. This matches the estimates from the previous calculations, confirming the theoretical foundation of using a discontinuous $\Upsilon(\vec{r})$.

5.1.2.3 Correctons with a changing $\Upsilon(\vec{r})$ in system 1

In a real time flux estimation, $\Upsilon(\vec{r})$ may have to be adjusted during a calculation. To test the method of adjusting the initial weight of the particles at the beginning of their history (section 4.3; Eq. (4.11)), a calculation has been performed where the value of $\Upsilon(\vec{r})$ flips between $\Upsilon^{(1)}(\vec{r})$ in the odd cycles and $\Upsilon^{(2)}(\vec{r})$ in the even cycles. They are characterised by $(\vec{\beta}^{(1)}_{i,j,k}, K^{(1)}_{i,j,k})$ and $(\vec{\beta}^{(2)}_{i,j,k}, K^{(2)}_{i,j,k})$ respectively. At the beginning of each cycle, the total weight of the particles is normalised to N^*.

The system has been divided in the same cells as in the previous section. The parameters are

$$\vec{\beta}^{(1)}_{1,1,k} = \begin{cases} \frac{1}{2}(\Sigma_T)\,\hat{z} & ,k = 1,\ldots,8 \\ 0 & ,k = 9,\ldots,16 \\ -\frac{1}{2}(\Sigma_T)\,\hat{z} & ,k = 17,\ldots,24 \end{cases} \tag{5.1}$$

and

$$\vec{\beta}^{(2)}_{1,1,k} = -\vec{\beta}^{(1)}_{1,1,k} \tag{5.2}$$

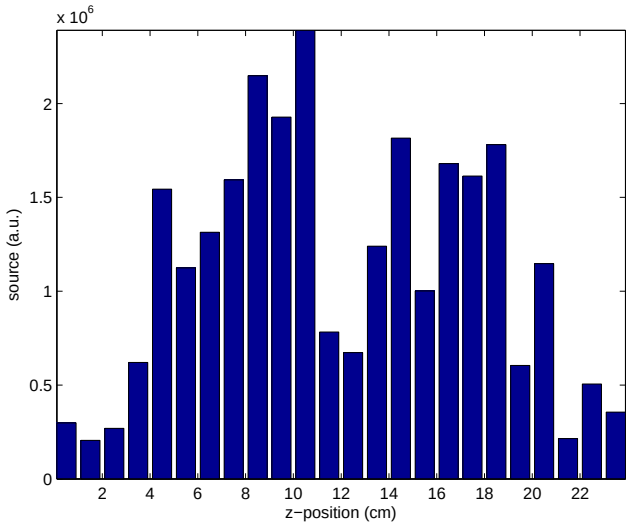

Figure 5.7: source distribution during active cycles of correcton calculation for a homogeneous rectangular parallelepiped (system 1) with a discontinuous, piece-wise constant $\Upsilon(\vec{r})$

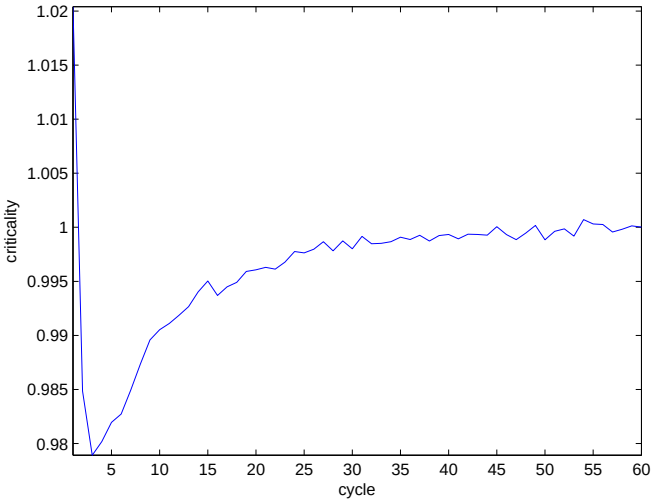

Figure 5.8: criticality estimates during inactive cycles of correcton calculation with a discontinuous, piece-wise constant $\Upsilon(\vec{r})$

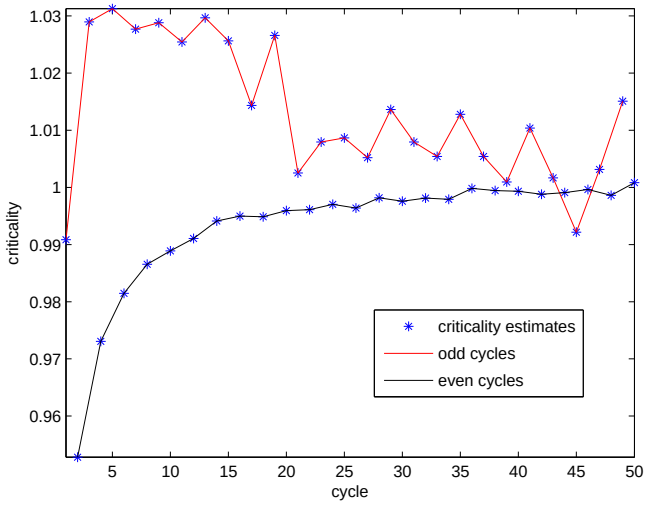

Figure 5.9: criticality estimates during inactive cycles of correcton calculation for a homogeneous rectangular parallelepiped (system 1); the value of $\Upsilon(\vec{r})$ is different in the even and the odd cycles.

respectively. In each case, values of $K^{(1)}_{1,1,k}$ and $K^{(2)}_{1,1,k}$ satisfy an equation similar to (4.18):

$$\frac{K_{1,1,k+1}}{K_{1,1,k}} = \exp\left[\left(C_{1,1,k}\vec{\beta}_{1,1,k} + C_{1,1,k+1}\vec{\beta}_{1,1,k+1}\right)\cdot\hat{z}\right] \ ,$$

where $C_{1,1,k} = \frac{1}{2}$ cm $\forall\ k$. (In this particular case, there are no discontinuities in $\Upsilon(\vec{r})$ at all.)

Note how $\Upsilon^{(1)}(\vec{r})$ and $\Upsilon^{(2)}(\vec{r})$ have a radically different shape. To avoid a very large variance amongst the initial weights of the particles in a cycle, the maximal length of the $\vec{\beta}_{1,1,k}$ is chosen to be $\frac{1}{2}\Sigma_T$.

In this calculation, $\mathcal{M} = 2\cdot 10^4$ and $N^* = 10^6$. The number of inactive cycles is 200.

The criticality estimates during the initial cycles are shown in Fig. 5.9. A line has been drawn through the odd and the even cycles. Note how they seem to converge at the same time, although they seem to be biased in a different direction during the initial cycles. Fig. 5.10 displays the criticality during some of the active cycles. The estimates in the odd cycles appear to have a far greater variance.

In each cycle, 500 particles were randomly selected and the positions and weights at the beginning of their histories were stored. Figures 5.12(a) and 5.12(b) show the particle distribution at the beginning of the histories in the active cycles for the odd and the even cycles. Figures 5.11(a) and 5.11(b) display the cumulative weight of all the particles in all the active cycles at different z-positions. That is, they display the shape of the source (which is also the shape of the flux $\mathcal{C}$).

Note the great similarities between figures 5.11(b) and 5.12(a) and between figures 5.11(a) and 5.12(b). This is quite easily explained by the fact that the

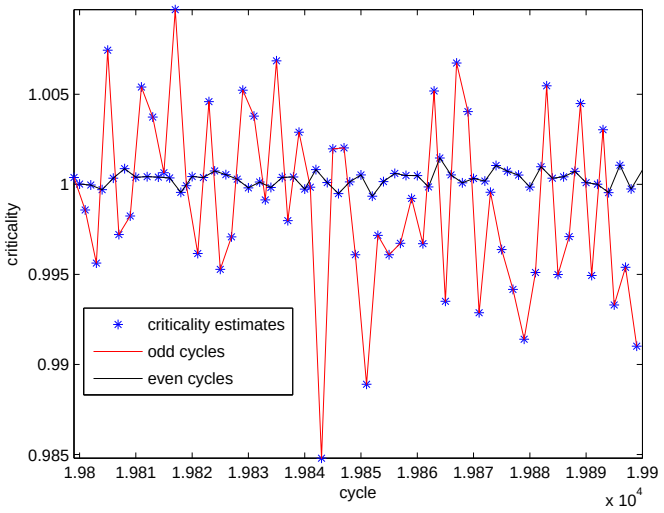

Figure 5.10: criticality estimates during some of the active cycles of correcton calculation for a homogeneous rectangular parallelepiped (system 1); the value of $\Upsilon(\vec{r})$ is different in the even and the odd cycles.

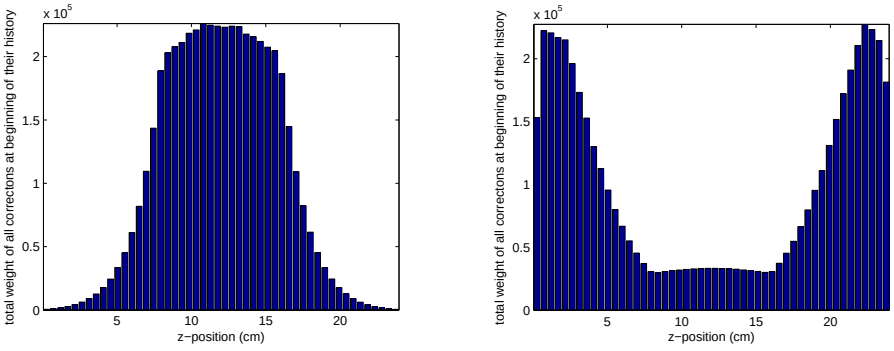

(a) odd cycles (b) even cycles

Figure 5.11: source distribution during a correcton calculation for a homogeneous rectangular parallelepiped (system 1); the value of $\Upsilon(\vec{r})$ is given by (5.1) in the odd cycles and by (5.2) in the even cycles

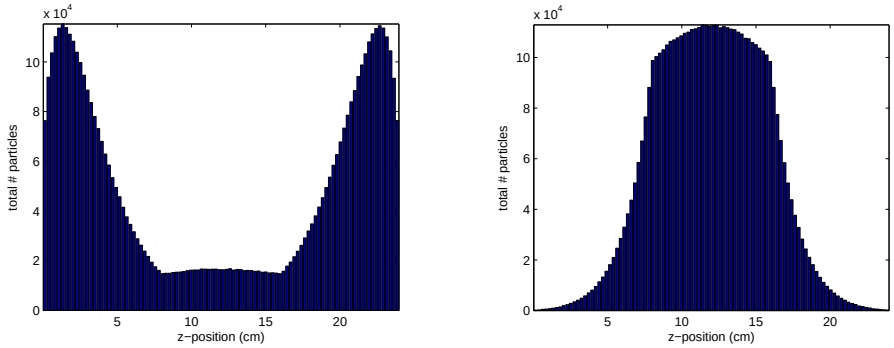

(a) odd cycles (b) even cycles

Figure 5.12: particle distribution during a correcton calculation for a homogeneous rectangular parallelepiped (system 1); the value of $\Upsilon(\vec{r})$ is given by (5.1) in the odd cycles and by (5.2) in the even cycles

particle distribution in an odd cycle is the result of a source distribution in an even cycle, and vice versa.

The difference in the variance of the criticality estimates can be accounted for by comparing the particle distributions (figures 5.12(a) and 5.12(b)). In the odd cycles, far more particles are situated near the edges of the medium and leak out of the system.

The criticality estimates are $k = 1.0001456$ on average. The error can be estimated based on the odd or the even cycles, leading to $4.8 \cdot 10^{-5}$ and $5.8 \cdot 10^{-6}$ respectively. This is consistent with the previously found values.

Note how the correctons have a completely different flux in every new cycle, yet the source seems to converge in about the same amount of cycles as in a neutron calculation. Apparently, the method of changing particle weights at the beginning of their history is very robust.

5.1.3 Real time flux estimation

The real time flux estimation methods proposed in sections 4.3, 4.4 and 4.5 are implemented for system 1. The system was divided into cubes with ribs of 1 cm, so there are 10 cells in the x-direction, 20 cells in the y-direction and 24 cells in the z-direction.

The neutron surface fluxes are determined in every cycle. In calculating the parameters for $\Upsilon(\vec{r})$ after cycle j, the average values of the surface fluxes over the last $\min(j, H)$ cycles are used. If there is some surface for which there have been no tallies in the last $\min(j, H)$ cycles, the calculation of $\Upsilon(\vec{r})$ is skipped.

Using equations similar to 4.16, the value of $\max\{m(a, b, c \to e, d, f)\}$ is also determined after every cycle and $\Upsilon(\vec{r})$ is only altered if $\max\{m\}$ is below some preset constant G.

At the beginning of every cycle, the total weight of the particles is normalised to N^*.

The parameters are $H = 20$, $G = 200$, $\mathcal{M} = 2 \cdot 10^4$ and $N^* = 10^6$. Fig. 5.13

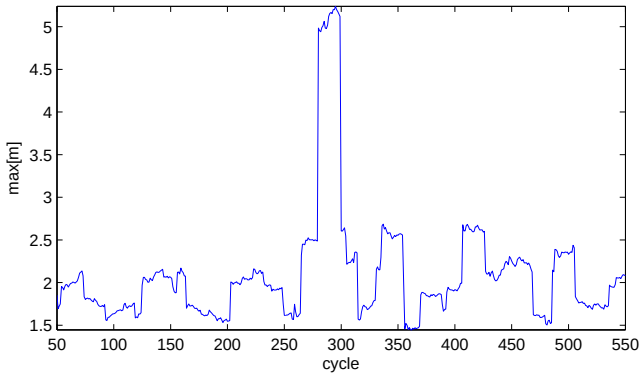

Figure 5.13: typical development of $\max\{m\}$ during some of the cycles of correcton calculation with real time neutron flux estimation for a homogeneous rectangular parallelepiped (system 1)

is a plot of the development of $\max\{m\}$ during some of the cycles. The value doesn't exceed 8.6 in any of the cycles. $\Upsilon(\vec{r})$ is therefore changed in every cycle.

The criticality estimate is $k = 1.000461 \pm 1.7 \cdot 10^{-5}$ with 100 inactive cycles.

In every cycle, 1500 particles were randomly selected and there position and weight was stored. From this, the source distribution in the active cycles was obtained. The source as a function of z only is shown in Fig. 5.14. The plots are very similar when the source is taken as a function of x or y only.

It can be seen that the source (and thus the flux) is almost constant, but it is a little greater near the edges of the medium. This probably indicates a very slight error in determining the correct $K_{i,j,k}$. It could be that an $\Upsilon(\vec{r})$ in the form of Eq. (4.9) is less suitable to describe the neutron flux near the edges of the system.

Remember that this does not pose a serious problem, since the choice of $\Upsilon(\vec{r})$ should not introduce a bias in the calculation (unless it is chosen in such an unfortunate way that the source iteration becomes unstable).

5.2 System 2: homogenised, loosely coupled fuel assemblies

5.2.1 Basic neutron calculation

A basic neutron calculation has also been performed for the second system. There were $\mathcal{M} = 1.2 \cdot 10^4$ cycles and $N^* = 10^5$ histories per cycle. A plot of the criticality estimations is shown in Fig. 5.15. It seems to converge after roughly 50 cycles. Fig. 5.16 shows how the criticality estimates are more or less constant during the active cycles. If the number of inactive cycles is taken to be 200, the average is $k = 0.9283358$ and the standard deviation of the average of the criticality estimates is $8.8 \cdot 10^{-6}$.

If, however, the source distribution plotted versus the cycles, it becomes apparent that the source doesn't converge at all. After each cycle, 500 particles

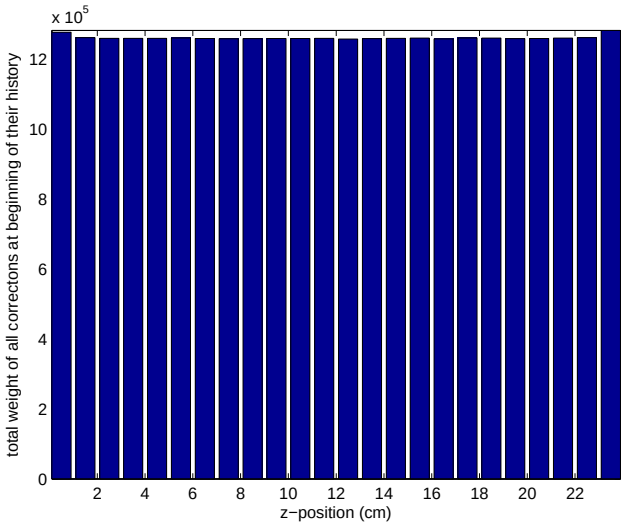

Figure 5.14: source distribution during the active cycles of correcton calculation with real time neutron flux estimation for a homogeneous rectangular parallelepiped (system 1)

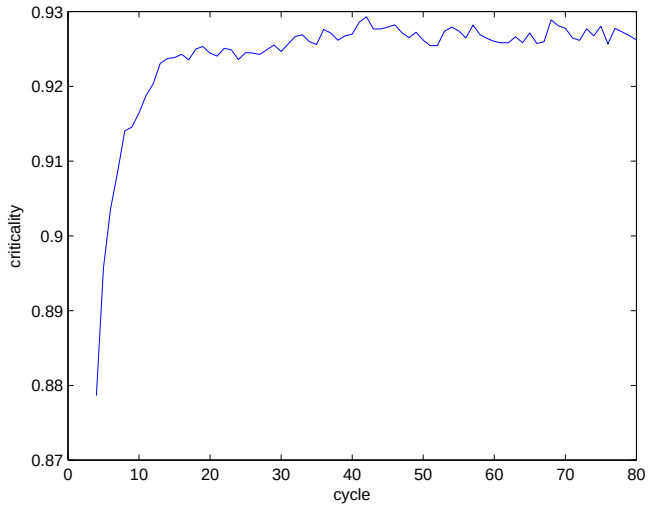

Figure 5.15: criticality estimates during inactive cycles of neutron calculation for loosely coupled fuel assemblies (system 2)

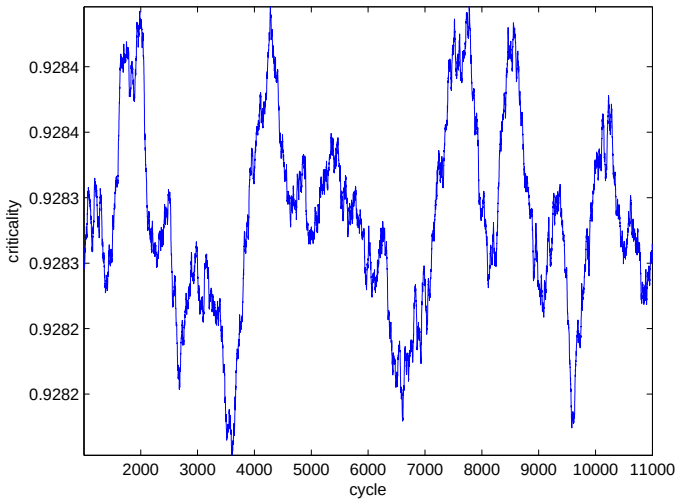

Figure 5.16: criticality estimates during some active cycles of neutron calculation for loosely coupled fuel assemblies (system 2) (smoothed with Savitzky-Golay filter of order 10^3)

were randomly selected and their positions were stored. Fig. 5.17 shows the number of particles in the different fuel assemblies versus the cycles. After 500 cycles, hardly any of the neutrons are present in the third and fourth fuel assembly. Even after many thousands of cycles, the source distribution is still altering in the other fuel assemblies.

The simulation has been repeated 6 times with $\mathcal{M} = 3 \cdot 10^3$ cycles. In each case, fuel assemblies 3 and 4 were quickly left with almost no neutrons. In some of the simulations, some of the other fuel assemblies emptied as well.

At first sight, it may seem strange that the neutrons have a tendency to pile up in the outer parts of the system. This is explained by the fact that the outer fuel assemblies (1,2,5 and 6) are surrounded by more concrete than the inner ones. Concrete has a much higher value of Σ_s/Σ_a. Therefore, neutrons that leak out of the fuel assembly have a higher probability of scattering back into the fuel.

It is interesting how the criticality estimate was consistently approximately $k = 0.9283$ throughout all realisations. Apparently it doesn't matter where the neutrons are in a criticality calculation. This is probably because the fuel assemblies are all equally shaped.

5.2.2 Real time flux estimation

A calculation similar to the one of section 5.1.3 has been done for the loosely coupled fuel assemblies of system 2. The number of cells in the x-, y- and z-direction are 8, 5 and 3 respectively. They are bounded by the planes $x = 0, 40, 70, 100, 115, 130, 160, 190, 230$, $y = 0, 40, 80, 120, 160, 200$ and $z = 0, 20, 100, 120$ (all values in cm.). This means that the outer fuel pins (1,2,5 and 6) consist of only one cell, whilst the inner fuel pins (3 and 4) consist of two equally shaped

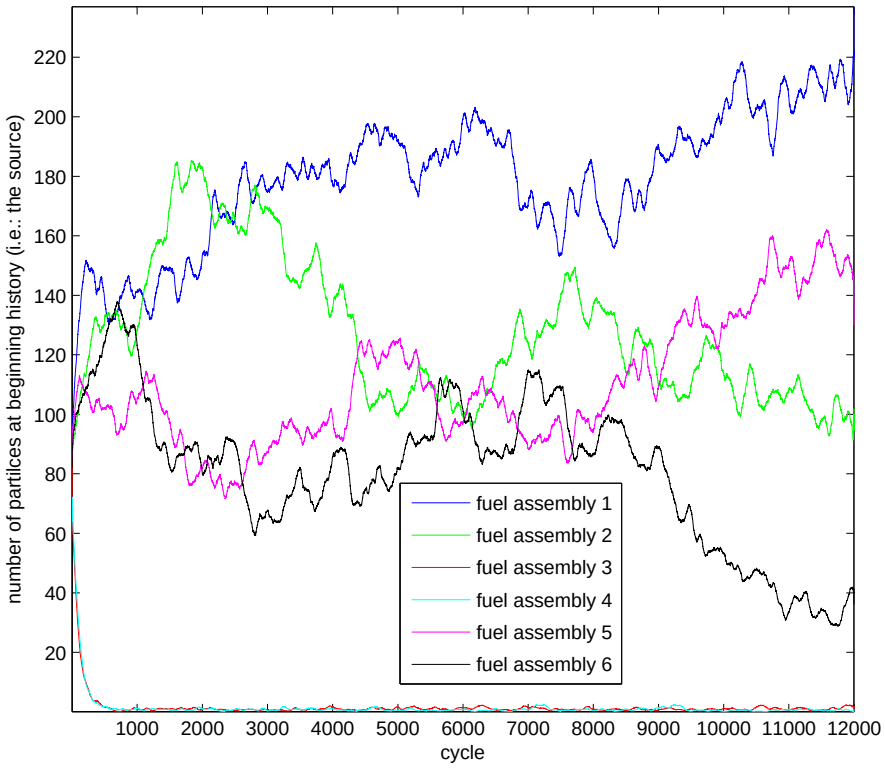

Figure 5.17: positions of 500 randomly selected particles at the beginning of their history in loosely coupled fuel assemblies (system 2), versus some of the active cycles (smoothed with moving average filter of order 80)

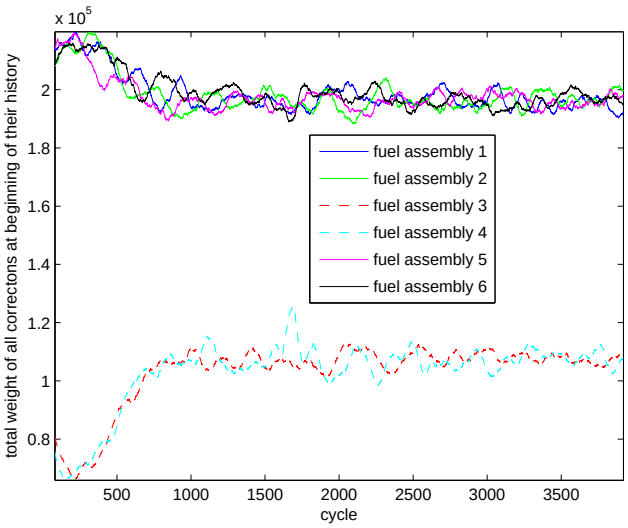

Figure 5.18: total weight of 1500 randomly selected particles at the beginning of their history versus some of the active cycles (smoothed with moving average filter of order 80) for the real time flux estimation of loosely coupled fuel assemblies (system 2)

cells that are located at different x-positions.

This time, the parameters were $H = 100$, $G = 200$, $\mathcal{M} = 4 \cdot 10^3$ and $N^* = 10^6$. The calculation has been done three times; the results were very similar in every respect.

The number of inactive cycles is 100; the criticality estimate is $k = 0.928217 \pm 2.8 \cdot 10^{-5}$.

In every cycle, 1500 particles were randomly selected and their properties at the beginning of their history were stored. The total weight of all particles in a fuel assembly is plotted in Fig. 5.18.

Fig. 5.19 is a plot of $\max\{m\}$ versus the cycle.

Since all fuel assemblies are of the same size, Fig. 5.18 clearly shows that the source, and thus also the flux, are far from homogeneous. However, there is a definite improvement over the conventional neutron calculation (Fig. 5.17). The inner fuel assemblies are not completely drained off particles and the outer fuel assemblies have a (more or less) constant source term.

Apparently, the real time flux estimation compensates to a significant degree for the destabilisation of the source convergence. This is quite a remarkable achievement, considering the fact that the fuel assemblies are separated by approximately a hundred mean free paths of a neutron.

The most probable explanation for the spatial variance in the correcton source is that there still aren't enough particles that can travel from the outer to the inner fuel assemblies to compensate for the difference in the multiplication factor.[2]

[2]For an alternative explanation, observe that the total correcton source in a fuel assembly

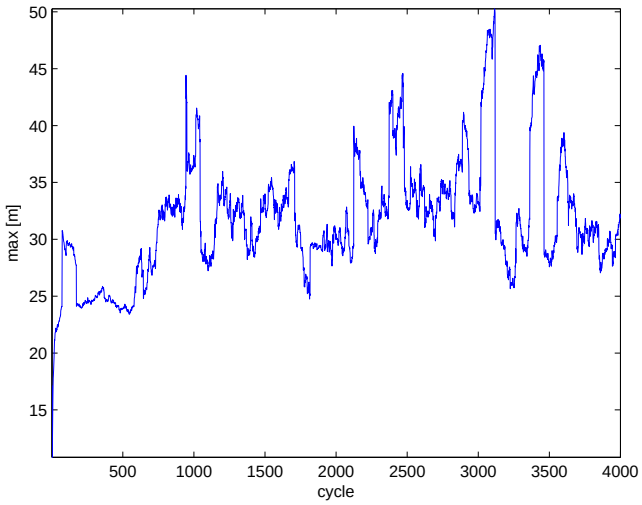

Figure 5.19: $\max\{m\}$ for all cycles of the real time flux estimation of loosely coupled fuel assemblies (system 2)

5.2.2.1 Two-dimensional flux estimation

The problems with source convergence are a result of a lack of communication between particles in the fuel pins in different x- and y-positions. In order for the source to converge, there is no need to even out the flux distribution in the z-direction.

Therefore, one might expect better results if $\vec{\beta}_{i,j,k} \cdot \hat{z} \equiv 0$, since Eq. (4.10) puts less of a restriction on $\vec{\beta}_{i,j,k} \cdot \hat{x}$ and $\vec{\beta}_{i,j,k} \cdot \hat{y}$. The exact same calculation as above has been performed with a slight modification of Eq. (4.13):

$$\vec{\beta}_{i,j,k} = \min\left(\frac{(\Sigma_T)_{i,j,k}}{\ell^*_{i,j,k}}, 1\right)\left[\frac{\ln\left(\frac{\mathcal{F}_{i^+,j,k}}{\mathcal{F}_{i^-,j,k}}\right)}{2A_{i,j,k}}, \frac{\ln\left(\frac{\mathcal{F}_{i,j^+,k}}{\mathcal{F}_{i,j^-,k}}\right)}{2B_{i,j,k}}, 0\right]^T ,$$

where

$$\ell^*_{i,j,k} \equiv \sqrt{\left(\frac{\ln\left(\frac{\mathcal{F}_{i^+,j,k}}{\mathcal{F}_{i^-,j,k}}\right)}{2A_{i,j,k}}\right)^2 + \left(\frac{\ln\left(\frac{\mathcal{F}_{i,j^+,k}}{\mathcal{F}_{i,j^-,k}}\right)}{2B_{i,j,k}}\right)^2} .$$

---

should be proportional to the total correcton flux, which is

$$\iint\limits_{<4\pi>}\left[\iiint\limits_{\text{fuel assembly}} \mathcal{C}\left(\vec{r},\hat{\Omega}\right)\,\mathrm{d}\vec{r}\right]\mathrm{d}\hat{\Omega} = \iint\limits_{<4\pi>}\left[\iiint\limits_{\text{fuel assembly}} \frac{\phi\left(\vec{r},\hat{\Omega}\right)}{\Upsilon\left(\vec{r}\right)}\,\mathrm{d}\vec{r}\right]\mathrm{d}\hat{\Omega}\ .$$

The exponential form of $\Upsilon\left(\vec{r}\right)$ is an extremely bad fit for the neutron flux within a fuel assembly. Therefore, the fact that $K_{i,j,k}$ was chosen to satisfy Eq. (4.19) is hardly a reason to believe that the rhs of the equation above will be the same for every fuel assembly (especially since the inner fuel assemblies consist of two cells, as opposed to the outer ones).

The value of $K_{i,j,k}$ can be adjusted in a similar manner to the one proposed in section 4.5.2. (Some of the calculations need a slight adjustment, since not all cartesian components of $\vec{\beta}_{i,j,k}$ are nonzero.)

A test showed no significant difference with the three-dimensional case. In this particular case, the fuel assemblies consist of only one cell in the z-direction, so $\mathcal{F}_{i,j,2^+} \approx \mathcal{F}_{i,j,2^-}$ and thus $\vec{\beta}_{i,j,2} \cdot \hat{z} \approx 0$ anyway.

5.2.2.2 Choice of the cell sizes

The first thing to note about the choice of the cell sizes is that the calculation time rapidly increases when more cells are used.

With other numerical methods that use grids in mind, it may seem tempting to choose smaller cells in the regions where one would expect a large divergence in the neutron flux (e.g. the boundary of a fuel assembly).

However, the tests from section 5.1.2 imply that this is not necessary to ensure source convergence inside a fuel pin, where there are no gabs between the regions where fission can occur. In systems like these, the problem is a lack of particles that travel large distances. To solve this, there is no need to be bothered by the flux distribution within a fuel assembly.

In fact, using smaller cells can easily lead to high discontinuities in Υ, completely destabilising the source convergence. This is mostly because far fewer particles will cross a small surface of a cell, resulting in large statistical variances in the estimation of the surface flux. This effect is even stronger if there are small cells near the boundary of a fuel assembly, where the neutron flux is low and its gradient is steep.

In the calculation above, the choice of cells can be adjusted to enhance the convergence. Because the inner fuel assemblies have two cells in the x-direction and the flux is higher in the centre, the correctons are pushed outward. The same calculation has been repeated with only one cell in each of the inner fuel assemblies.

A plot of the resulting total correcton sources in the fuel assemblies (similar to Fig. 5.18) is shown in Fig. 5.20. After some cycles, the total source (and thus the total flux) is equal for all fuel assemblies.

With 900 inactive cycles, the criticality is estimated to be $k = 0.928401 \pm 4.1 \cdot 10^{-5}$.

A peculiar detail in the calculation is that the total correcton source in fuel assembly 1 suddenly increases by a factor of 1.5 after cycle 5657. Possibly there is a single particle that gained a very large weight. The particles gradually even out again over the next 50 to 100 cycles.

5.3 Other tests

The correcton method has been tested for several systems with loosely coupled fuel assemblies, similar to system 2. For example, in one test the concrete has been made a good absorber, so it doesn't scatter the particles back into the fuel assemblies. In another simulation, there were more fuel assemblies with less symmetry in the system. Several tests have also been done with a far lower number of simulated histories per cycle (in the order of 10^4).

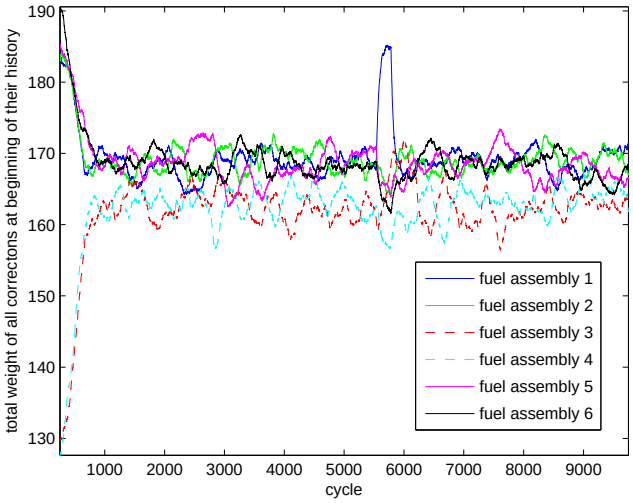

Figure 5.20: source in different fuel assemblies for a new real time flux estimation (smoothed with moving average filter of order 250); compare with Fig. 5.18

In every case, the correctons converged to a more or less uniform distribution. The method seems to work well, so long as all the fuel assemblies and the spaces in between consist of only one cell.

Chapter 6

Conclusion

A self-learning correcton method has the potential of solving some of the source convergence problems present in conventional Monte Carlo calculations. The greatly reduced spatial variance of the particle distribution should also make estimating the flux at different locations in a system simultaneously more efficient.

Other advantages include:

- No prior calculations are necessary.
- It is often easy to verify that the source iteration has converged and isn't trapped in some local minimum. After convergence, the flux should have hardly any spatial variation.
- As opposed to a (relatively) more conventional correcton calculation, very little expertise or physical insight is needed. However, one still has to choose the grid cells correctly.

When choosing the size of the grid cells, there are several issues to take into account. Although it may seem counter-intuitive, the relative discontinuities in $\Upsilon(\vec{r})$ are smaller if larger cells are used. This is mostly because there are more particles crossing a cell boundary, resulting in more accurate estimations of the average flux over the boundary. As a general rule of thumb, one should not be too bothered by the specific shape of the neutron flux within a fuel assembly. The correctons only have to directed on a larger scale, in such a way that there is as much interaction as possible between loosely coupled systems.

The choice of $K_{i,j,k}$ from section 4.5.2 seems to work quite well. Fig. 5.19 seems to suggest that the discontinuities in the flux estimate are not particularly troublesome. A noticeable deviation from a constant flux is visible in Fig. 5.14, but since it is very small, it can simply be ignored.

Chapter 7

Future work

The logical next step is to implement a real time flux estimation technique in a commercial Monte Carlo code that either has problems with source convergence, or where the flux has to be estimated in different regions of a system. (This has never been done for the correcton method in general.) This will require several generalisations, such as particles that can have any energy and delayed neutrons.

There are also some possible refinements to the methods described here, some of which are listed below.

- The flux estimate during a calculation is based on tallies from some of the last cycles, where each cycle has been given an equal weight. The source might converge faster if they are weighted and tallies from later cycles are given a greater weight.
- The correcton method in general remains untested for a more general three-dimensional geometry, where not all cells are rectangular parallelepipeds. This will probably make it more difficult to find a good way to adjust the parameters of the neutron flux estimate.
- In this thesis, attention has only been paid to the maximal theoretically possible weight change for a particle that crosses from one cell to another. This is a rather crude measure. For example, the region with a large relative discontinuity in $\Upsilon(\vec{r})$ might well be quite small, thus hardly endangering the stability of the calculation.

It might also be interesting to investigate how the correlation between estimates of quantities in different cycles is effected by the real time correcton method. It could be that the positions of the particles are less positively correlated, especially if the neutron flux estimate is based only on the last cycle. This could make it easier to determine the error in the final estimate of the quantity.

Appendix A

Notes on stochastics

A.1 Probability and random variables

Intuitively, a stochastic variable is a variable whose value cannot be determined in advance. The mathematical formalisation of this concept requires the notion of a **probability space** $(\mathcal{O}, \mathcal{H}, \mathcal{P})$, which is defined by the following properties. (Kroese et. al. [9], 605-606)

1. $\mathcal{O}$ is the set of all possible values of the stochastic variable, called the **sample space**.
2. $\mathcal{H}$ is the σ-field of all events. An **event** is a subset of $\mathcal{O}$ to which a probability can be assigned. A **σ-field** $\mathcal{H}$ is a collection that satisfies the following properties:
   (a) $\mathcal{H} \neq \emptyset$;
   (b) $A_1, A_2, \ldots \in \mathcal{H} \Rightarrow (A_1 \cup A_2 \cup \ldots) \in \mathcal{H}$;
   (c) $A \in \mathcal{H} \Rightarrow A^{\mathrm{c}} \in \mathcal{H}$.
3. $\mathcal{P}$ is a **probability measure** that assigns a number $\mathcal{P}(A)$ to every $A \in \mathcal{H}$. It must satisfy the **Kolmogorov axioms**[1]:
   (a) **nonnegativity**: $\mathcal{P}(A) \geq 0 \ \forall \ A \in \mathcal{H}$;
   (b) **unit measure**: $\mathcal{P}(\mathcal{O}) = 1$;
   (c) **sum rule**: $A_i \cap A_j = \emptyset \ \forall \ i, j \Rightarrow \mathcal{P}\left(\bigcup_x A_x\right) = \sum_x \mathcal{P}(A_x)$.

   $\mathcal{P}(A)$ is said to be the **probability** of A.

An event A happens **almost surely** if and only if $\mathcal{P}(A) = 1$.[2]

[1] Sometimes the more intuitive Cox's theorems are used instead, but they make argument that transforms equation (3.8) in section 3.2 into a Markov process more difficult.

[2] This terminology is used when there are several theoretical outcomes, but only one of them doesn't have a vanishingly small probability. (For example, when tossing a coin 10^{100} times, there's a probability of $\left(\frac{1}{2}\right)^{\left(10^{100}\right)}$ that none of the tosses will be a tails. But when the coin is tossed an infinite number of times, there will almost surely be a tails at least once.)

Formally, a stochastic variable X that takes on values in some set E (called the **state space**) is a function $X : \mathcal{O} \to E$ such that

$$\{X \in B\} \equiv \{\gamma \in \mathcal{O} | X(\gamma) \in B\} \in \mathcal{H} \; \forall \; B \in \mathcal{E} \; , \tag{A.1}$$

where $\mathcal{E}$ is a σ-field on E. If E is countable, then X is called **discrete**, otherwise it's called **continuous**. (Kroese et. al. [9], 607-609)

Somewhat heuristically, the **probability distribution** is a function that describes the probability that $X \in B$ for all B. If X and Y are stochastic variables, the statement '$X \sim Y$' denotes that X has the same probability distribution as Y. If X is defined by (A.1) on a well-defined probability space, then all the usual properties of its probability distribution will hold.

Define the **probability operator** $\mathbb{P}[-]$ as follows:

- If $\mathcal{S}$ is a statement, $\mathbb{P}[\mathcal{S}]$ is the probability that $\mathcal{S}$ is true.
- If $\mathcal{D}$ is a discrete stochastic variable (that is, if E is countable), then $\mathbb{P}[\mathcal{D}](z) \equiv \; \mathbb{P}[\mathcal{D} = z]$.
- If $\mathcal{C}$ is a continuous stochastic variable in the hyperspace $\mathbb{R}^n$, then $\mathbb{P}[\mathcal{C}](z) \equiv V^{-1}\mathbb{P}[z \in \mathcal{V}]$, where $z \in \mathbb{R}^n$, $\mathcal{V}$ is some vanishingly small part of $\mathbb{R}^n$ about z and V is the volume of $\mathcal{V}$.

In the last case, $\mathbb{P}[\mathcal{C}]$ is the **probability density** function of $\mathcal{C}$. If X can take on values in the uncountable set $\mathbb{R}^n$, it is quite possible that $\mathcal{P}(X = \alpha) = 0 \; \forall \; \alpha \in \mathbb{R}^n$, whilst not violating the unit measure Kolmogorov axiom. However, the probability density will in general still be positive. From the Kolmogorov axioms it follows that $\mathbb{P}[\mathcal{C}] \in \mathbb{R}^+$ and $\int_{R^n} \mathrm{d}z \; \mathbb{P}[\mathcal{C}](z) = 1$.

A.2 Markov chains and MCMC

A set J is called an **index set** of A if there is a surjective function from J to A. A **stochastic process** is a set of random variables $\{X_\tau\}$ on a probability space $(\mathcal{O}, \mathcal{H}, \mathcal{P})$ where τ is in any index set J. It is often helpful to view τ as the time and X_τ as a random variable that is evolving through time.

A **Markov process** is a stochastic process that satisfies the **Markov property**:

$$(X_{t+s} | X_u, u \leq t) \sim (X_{t+s} | X_u, u = t) \; \forall \; s \geq 0 \; .^3$$

The Markov property is sometimes called '**memorylessness**'. In words, it can be interpreted as a stochastic process for which, conditional on its 'present' state, the 'past' and the 'future' are independent.

In this thesis, only processes with the index set $\mathbb{N}$ are considered. Since the index set is countable, the process is called a **Markov chain**. The state space will be in $\mathbb{R}^n$.

The **transition kernel** P_s is a function defined as

$$P_s(x, A) = \mathbb{P}[X_{t+s} \in A | X_t = x] \; .$$

[3] Note this is a **conditional** probability density. (ref. Dekking et al. [7], chapter 3 or Kroese et al. [9], pages 618-619))

It is the probability that X_t will 'evolve' from x to some value in A in s time steps. It can usually be written as

$$P_s(x, A) = \int_A p_s(x, y)\ \mathrm{d}y,$$

where $p_s(x, y)$ is the **transition density**. All Markov processes will be considered to be **time-homogeneous**, meaning that the transition kernel, and thus the transition density, do not depend on the time. (Kroese et. al. [9], 628)

The product rule for probabilities leads directly to the **Chapman-Kolmogorov** equations:

$$p_{a+b}(x, y) = \int_{q \in E} p_a(q, y)\ p_b(x, q)\ \mathrm{d}q\ .$$

Also, if f_0 is the joint probability density function[4] of some Markov chain $(R_0, R_1, \ldots, R_n)$, then

$$f_n(r_0, r_1, \ldots, r_n) = f_0 \prod_{i=1}^{n-1} p_1(r_n, r_{n+1})\ .$$

If certain requirements are met (Kroese et. al. [9], 630-635), there will be a **limiting distribution** π such that

$$\lim_{t \to \infty} p_t(x, y) = \pi(y)\ . \tag{A.2}$$

Under certain conditions, existence of the limiting distribution implies its uniqueness and it can be determined as the solution to the set of equations

$$\begin{aligned} \pi(y) &= \int \pi(x) p_s(x, y)\ \mathrm{d}x\ \forall\ s \in \mathbb{N}\ , \\ \int \pi(y)\ \mathrm{d}y &= 1\ . \end{aligned} \tag{A.3}$$

In other words, π is the **stationary distribution** of the Markov chain.

In a Monte Carlo calculation, it may often be difficult to sample from a probability distribution f if it cannot be written in a closed form. Though it may seem surprising, it is often still possible to find some time-homogeneous Markov chain of which it is known that it has f as its stationary distribution. The transition kernel of this Markov process for a unit time step is usually quite simple to sample from.

The goal of the **Markov chain Monte Carlo** (**MCMC**) method is to generate *approximate* samples from some stationary distribution π in Eq. (A.2). This can be done using the **power method**. To this end, pick some starting value X_0 and use the unit time step transition kernels to generate a Markov process $\{X_0, X_1, \ldots\}$. The idea is that, for some $M > 0$, X_M will have a similar probability distribution as π. It can thus be used to draw an approximate sample from π.

[4] ref. Dekking et al. [7], chapter 9

Appendix B

Sampling stochastic variables

B.1 Pseudorandom numbers

A computer program performs a set of prescribed actions. It is incapable of doing something at random. For Monte Carlo calculations however, it is necessary to sample random variables. To facilitate this, modern programming languages are equipped with an algorithm to sample **pseudorandom** numbers from a uniform distribution from 0 to 1. The algorithm generates a sequence of numbers that approximates the properties of random variables. The sequence isn't truly random, but is determined by a (small) set of variables (the **seed**) that has to be specified. The seed should be chosen at random.

Since a computer can only store a finite amount of unique variables in the set $(0, 1)$, the sequence of pseudorandom numbers will be repetitive. The **period length** is the largest number of samples that can be drawn from a pseudorandom number generator without the guarantee that the sequence is repetitive.

For a more formal discussion of random number generation, the reader is referred to Kroese, et al. [9], chapter 1. A few basic requirements for random number generators are also stated there. Amongst others, they should not return the values 0 or 1 and the stream of pseudorandom numbers should be reproducible. Also, the period length should at least be of the order of $\max(10^{50}, 10N^2)$, where N is the number of generated numbers. Most older random number generators didn't meet this last demand.

For the calculations in this thesis, the seed was sometimes chosen in such a way that the results are reproducible. In other occasions it was based on the CPU-time of the computer at the start of the calculation. The period after which the pseudorandom sequence repeats itself is considered to be large enough to avoid practical problems. The random number generator is assumed to work perfectly.

B.2 Sampling from a known probability density

A computer will usually only sample from a uniform distribution from 0 to 1. The following procedure can be used to sample values of a random variable X with an arbitrary probability density function $f(z)$. (To see *why* this works, a plot of a random cumulative probability density function should suffice. See, for instance, Dekking et al. [7], pages 72-73.)

Determine

$$\mathbb{P}\left[X < z\right] = F(z) \equiv \int_{-\infty}^{z} f(s)\mathrm{d}s \tag{B.1}$$

and note that $F(z)$ is monotonically increasing function of z and $0 \leq F \leq 1$. Now define F^{-1} as the inverse of F.[1] Suppose a uniformly distributed random number $\rho \in (0, 1)$ has been obtained. If the random variable k is defined by

$$k = F^{-1}(\rho),$$

it has a probability density function of f.

For example, Eq. (3.9) can be found by taking f to be equal to the exponential distribution of Eq. (2.3). Then, from Eq. (B.1), $F(d) = 1 - \exp\left(-\Sigma_T d\right)$ and thus $F^{-1}(\rho) = -\frac{1}{\Sigma_T}\ln\left(1-\rho\right)$. Finally, observe that $(1-\rho) \sim \rho$.

Discrete random variables can be viewed as continuous variables with a probability density function that consists of a train of Dirac delta functions δ. Specifically, if a stochastic variable Y has the possible values $y_1, y_2, \ldots, y_N$ with respective probabilities $p_1, p_2, \ldots, p_N$ such that $y_1 < y_2 < \ldots < y_N$, then it can be treated as a continuous stochastic variable with a probability density function

$$\mathbb{P}\left[Y\right](u) = \sum_{i=1}^{N} p_i \ \delta(u - y_i).$$

Thus the cumulative probability density function is

$$\mathbb{P}\left[Y < u\right] = \int_{-\infty}^{u} \mathbb{P}\left[Y\right](s) \ \mathrm{d}s = \sum_{i=1}^{N} p_i \ \mathrm{H}(u - y_i),$$

where H is the Heaviside function. The inverse can easily be determined graphically and this leads to the result that Y can be sampled by

$$y_1 + \sum_{i=1}^{N-1} \left[(y_{i+1} - y_i) \ \mathrm{H}\left(\rho - \sum_{j=1}^{i} p_j \right) \right].$$

(Again, ρ is a uniformly distributed stochastic variable.)

An application of this procedure would be to sample the amount of new neutrons after a fission reaction.

One can also randomly select events by attributing a unique number to each event and following the procedure for sampling discrete stochastic variables.

[1] $F(z)$ may not be *strictly* monotonically increasing for all z. On those parts of the domain where it isn't, $F^{-1}(z)$ may not be unambiguously defined, but this is not a problem.

Sometimes the methods described above can be very difficult or computationally expensive. Kroese et al. [9], 85-224, provides the most efficient algorithms to sample from most well-known probability densities. They are usually based on some specific characteristics of the distributions.

B.3 Sampling an isotropic direction vector

If a unit vector $\hat{\Omega}$ is placed at the origin, it will point to some point on the surface of the unit sphere around the origin. If it has a random isotropic direction, the probability that it will point to some part of the surface is proportional to the area of that part of the surface. Define the Cartesian coordinates x, y and z and $\Omega_i \equiv \hat{\Omega} \cdot \hat{i} \; \forall \; i \in \{x, y, z\}$. The probability that $z < \Omega_z < z + \mathrm{d}z$ is proportional to the area of a unit sphere between z and $z + \mathrm{d}z$.

This area can be calculated as the 'rotational area'[2] of the function $y = \sqrt{1 - z^2}$ about the z-axis. In general, the length of a surjective function $y = y(x)$ between x and $x + \mathrm{d}x$ is

$$\sqrt{\mathrm{d}x^2 + \mathrm{d}y^2} = \sqrt{1 + \left(y'(x)\right)^2}\ \mathrm{d}x\ .$$

Putting everything together,

$$\mathbb{P}\left[z < \Omega_z < z + \mathrm{d}z\right] = \frac{\left(2\pi \cdot \sqrt{1 - z^2}\right)\left(\sqrt{1 + \left(\frac{\mathrm{d}}{\mathrm{d}z}\left(\sqrt{1 - z^2}\right)\right)^2}\mathrm{d}z\right)}{\text{(total area of the unit sphere)}} = \frac{1}{2}\mathrm{d}z$$

for all $z \in (-1, 1)$.

Using spherical coordinates and denoting the polar and azimuth angles by ϑ and γ, any book on calculus will tell you that

$$(\Omega_x,\ \Omega_y,\ \Omega_z) = (\sin\vartheta\ \cos\gamma,\ \sin\vartheta\ \sin\gamma,\ \cos\vartheta)\,. \tag{B.2}$$

Therefore $\cos\vartheta$ can be sampled from a uniform distribution from -1 to 1. Because of symmetry, it is obvious that γ has a constant probability density function with a width of 2π.

Using Eq. (B.2) in combination with some trigonometric identities, the cartesian components of an isotropic unit vector can now be sampled by

$$\begin{aligned}
\Omega_x &= 2\sqrt{\zeta_1\,(1 - \zeta_1)}\ \cos(2\pi\zeta_2), \\
\Omega_y &= 2\sqrt{\zeta_1\,(1 - \zeta_1)}\ \sin(2\pi\zeta_2), \\
\Omega_z &= 2\zeta_1 - 1,
\end{aligned}$$

where ζ_1 and ζ_2 are independent and uniformly distributed from 0 to 1.

[2] the area of the surface of the solid that is generated by revolving a function around an axis

Appendix C

System specifications

C.1 System 1: simple bar

This system consists of a homogeneous rectangular parallelepiped in an infinite vacuum. If x, y and z are the cartesian coordinates, then the bar is bounded by the planes $x, y, z = 0$ cm, $x = 10$ cm, $y = 20$ cm and $z = 24$ cm. The macroscopic cross sections are $\Sigma_T = 1.0000$ cm^{-1}, $\Sigma_a = 0.5882$ cm^{-1} and $\Sigma_f = 0.2500$ cm^{-1}. The average number of new neutrons produced in a fission reaction is $\nu = 2.5$.

The system is very nearly critical.

C.2 System 2: fuel assembly # 1

The system consists of a rectangular parallelepiped medium surrounded by an infinite vacuum. Denote the cartesian coordinates by x, y and z and take one of the corners of the parallelepiped to be the origin. Define the length $l \equiv 1$ cm and $x^* \equiv x/l$, $y^* \equiv y/l$ and $z^* \equiv z/l$.

The medium consists of three different materials: water, concrete and six equally shaped fuel assemblies. Let F, W and C be the regions where there is fuel, water or concrete respectively. The i^{th} fuel assembly is in F_i.

The composition of the medium is given by

$$\begin{aligned}
F_1 \equiv &\quad \{x, y, z \in \mathbb{R}^3 | \quad 040 < x^* < 070 \wedge 040 < y^* < 080 \wedge 020 < z^* < 100\} \ ; \\
F_2 \equiv &\quad \{x, y, z \in \mathbb{R}^3 | \quad 040 < x^* < 070 \wedge 120 < y^* < 160 \wedge 020 < z^* < 100\} \ ; \\
F_3 \equiv &\quad \{x, y, z \in \mathbb{R}^3 | \quad 100 < x^* < 130 \wedge 040 < y^* < 080 \wedge 020 < z^* < 100\} \ ; \\
F_4 \equiv &\quad \{x, y, z \in \mathbb{R}^3 | \quad 100 < x^* < 130 \wedge 120 < y^* < 160 \wedge 020 < z^* < 100\} \ ; \\
F_5 \equiv &\quad \{x, y, z \in \mathbb{R}^3 | \quad 160 < x^* < 190 \wedge 040 < y^* < 080 \wedge 020 < z^* < 100\} \ ; \\
F_6 \equiv &\quad \{x, y, z \in \mathbb{R}^3 | \quad 160 < x^* < 190 \wedge 120 < y^* < 160 \wedge 020 < z^* < 100\} \ ,
\end{aligned}$$

$$F = F_1 \cup F_2 \cup F_3 \cup F_4 \cup F_5 \cup F_6 \ ,$$

$$W = \{x^*, y^*, z^* \in \mathbb{R}^3 | 40 < x^* < 190 \wedge 40 < y^* < 160 \wedge 20 < z^* < 100\} \setminus F$$

and

$$C = \{x^*, y^*, z^* \in \mathbb{R}^3 | 0 < x^* < 230 \wedge 0 < y^* < 200 \wedge 0 < z^* < 120\} \setminus \{F \cup W\} \ .$$

Note how there is at least 30 centimetre of space between every fuel assembly.

The values of the cross sections and the average amount of new particles in a fission reaction are tabulated below. The neutrons can have only one energy. There are no delayed neutrons.

	fuel	water	concrete
Σ_T (cm^{-1})	1.150	3.000	0.350
Σ_a (cm^{-1})	0.025	0.300	0.0029
Σ_f (cm^{-1})	0.011	0.000	0.000
ν $(-)$	2.4545	0.000	0.000

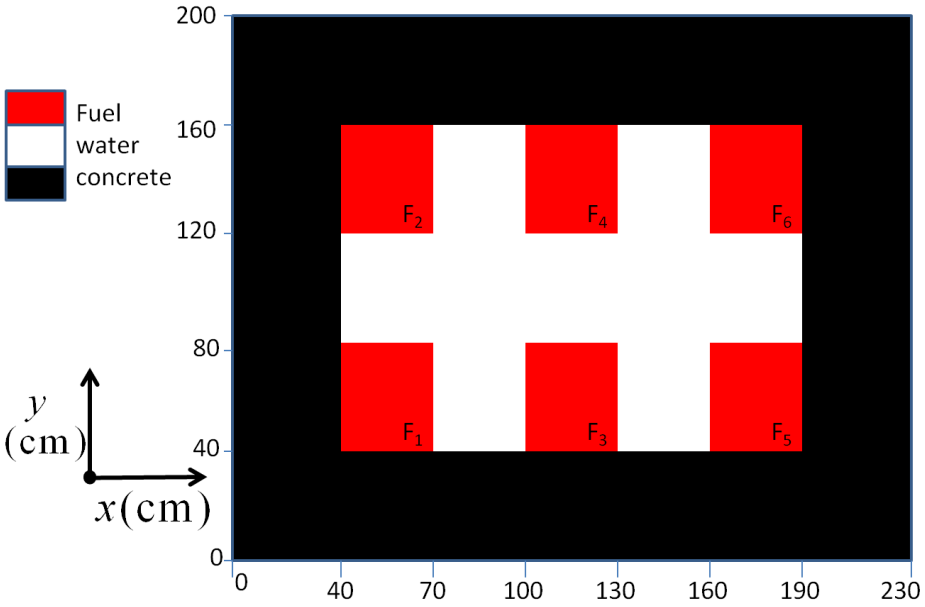

Figure C.1: sketch of the cross section of system 2 at a plane perpendicular to the z-axis anywhere in the region 20 cm $< z <$ 100 cm

Bibliography

[1] Hoogenboom, J. E., Sjenitzer, B. L.: *Monte Carlo Lectures*, PNR, R^3, TNW, TU Delft (2011)

[2] Duderstadt, J. J., Hamilton, L. J.: *Nuclear Reactor Analysis*, Wiley (1976), Department of Nuclear Engineering, The University of Michigan

[3] Bowler, M. G.: *Nuclear Physics*, Pergamon Press (1973)

[4] Sjenitzer, B.: *Variance Reduction Using The Correcton Method on Criticality Calculations*, TU Delft, PNR (2009)

[5] Becker, T. L., Wollaber, A., B., Larsen, E. W.: *A Hybrid Monte Carlo-Deterministic Method for Global Particle Transport Calculations*, University of Michigan, Department of Nuclear Engineering and Radiological Sciences (2006)

[6] Becker, T, L.: *Hybrid Monte Carlo/Deterministic Methods for Radiation Shielding Problems*, Nuclear Engineering and Radiological Sciences, University of Michigan (2009)

[7] Dekking, F. M., Kraaikamp, C., Lopuhaä, H. P., Meester, L. E.: *A Modern Introduction to Probability and Statistics, Understanding Why and How*, Springer texts in statistics (2009), applied mathematics, TU Delft

[8] Huisman, M., V.: *variance reduction in a three dimensional space using the correcton method*, TU Delft, PNR (2011)

[9] Kroese, D. P., Taimre, T., Botev, Z. I.: *Handbook of Monte Carlo Methods*, Wiley series in probability and statistics (2011)